RSC Sustainability

ROYAL SOCIETY OF CHEMISTRY

CRITICAL REVIEW

View Article Online
View Journal | View Issue

Cite this: *RSC Sustainability*, 2026, **4**, 1203

Application of MXenes for emerging contaminant removal and water purification: a revolutionary approach

Savan K. Raj, *[a] Prem P. Sharma,[b] Dominika Bury, [d] Agnieszka M. Jastrzebska[d] and Vaibhav Kulshrestha*[c]

Received 21st May 2025
Accepted 29th December 2025

DOI: 10.1039/d5su00364d

rsc.li/rscsus

Emerging water contaminants, including dyes, heavy metals, pharmaceuticals, per- and poly-fluoroalkyl substances (PFAS), and micro- and nano-plastics, pose critical challenges for environmental sustainability and human health. Two-dimensional transition metal carbides and nitrides (termed as MXenes) have recently emerged as transformative materials for water purification owing to their high surface area, tunable chemistry, electrical conductivity, and photocatalytic activity. This review summarizes the latest advances in MXene-based adsorbents, membranes, and hybrid composites, elucidating the mechanistic underpinnings for adsorption, electrosorption, photocatalysis, and ion-exchange processes. Regeneration strategies, recyclability, and long-term stability are critically assessed, alongside the potential environmental and human health risks posed by MXenes and their degradation products. Key challenges in the scalable synthesis, structural stability, and membrane integration are highlighted, and strategies for mitigating toxicity and optimizing performance are proposed. The insights presented provide a roadmap for the design of next-generation, sustainable MXene-enabled water purification technologies.

Sustainability spotlight

This review evaluates the high-efficiency contaminant removal capabilities of MXenes and critically examines the green synthesis pathways, reproducibility challenges, and environmental risks associated with their use. By integrating performance insights with sustainability, safety, and scalability considerations, it provides a roadmap for responsibly translating MXene-based technologies into practical, real-world water purification solutions.

1 Introduction

The rapid expansion of urban areas, combined with global population growth, has increased the demand for sufficient supplies of clean water.[1] In addition, the rapid pace of urbanization has contributed to the generation of toxic waste, posing significant risks to human health and environment.[2] The existence of contaminants like salts, heavy metal ions, pharmaceuticals, perfluoroalkyl and polyfluoroalkyl substances (PFAS), dyes, and aromatic compounds in aqueous media or wastewater streams creates an environmental concern because most of them are toxic and highly hazardous for all living organisms.[3] Various methods, *i.e.*, biological and physicochemical, which include aerobic/anaerobic digestion, biochar treatment,[4,5] adsorption,[6] and membrane filtration,[7] are traditionally executed for the remediation of different environmental pollutants. Moreover, nanomaterials, as catalytic/antibacterial agents, adsorbents, and membranes with different functionalities, have become economically feasible and eco-friendly choices for methodical contaminant elimination in water and wastewater management.[8] Zeolites, ceramics, carbon nanostructures, and metal–organic frameworks (MOFs) are some of these advanced functional nanomaterials. Structuring nano-based material devices may enable us to achieve unique levels of selectivity, mechanical stability, sensitivity, and efficiency in pollutant removal processes.[9] Two-dimensional (2D) nanomaterials are characterized by atomic-scale thickness and lateral dimensions ranging from tens of nanometres to several micrometres.[10] The nanometer-scale thickness provides these materials with exceptional properties like high surface areas, making them fascinating candidates for environmental remediation applications like catalysis, sensing, and adsorption.[11] So far, in the field of contaminant remediation, graphene-based

[a]*Institut National De Recherche Scientifique (INRS), Energie Materiaux Telecommunications, 1650 Lionel-Boulet Blvd., Varenners, Quebec, J3X 1P7, Canada. E-mail: savankraj@gmail.com*

[b]*Cergy Paris University, Cergy, 95000, France*

[c]*CSIR-Central Salt and Marine Chemicals Research Institute, Gijubhai Badheka Marg, Bhavnagar 364 002, Gujarat, India. E-mail: Vaibhavphy@gmail.com*

[d]*Faculty of Mechatronics, Warsaw University of Technology, św. A. Boboli 8, 02-525 Warsaw, Poland*

nanomaterials have shown great potential as adsorbents and photocatalytic materials as well as in membrane separation and sensing.[12] In addition, graphene and its derivatives have shown extraordinary performance in membranes for the water purification process.[13] In the class of 2D materials, GO and its derivatives have been predominantly studied for the removal of various contaminants.[14–16]

MXenes have been introduced as a new class of 2D nano-based materials that have originated from the family of transition metals carbides, carbonates, and nitrides, and they are generally denoted by the formula $M_{n+1}X_nT_x$ (n = 1, 2, and 3), where M stands for the early transition metal group, X stands for carbon or nitrogen, and T_x stands for the attached surface terminal groups (like –OH, –F or –O);[17] the materials used to build MXenes are shown in Fig. 1a. These MXenes are synthesized by their respective MAX phases, which are denoted by the general formula $M_{n+1}AX_n$, where M represents a transition metal, A is an A-group element (typically IIIA and IVA; *e.g.*, Al, Si, and Ga), X denotes C and/or N, and n ranges from 1 to 3. The synthesis process entails the removal of the "A" atom from the middle layer using various methods. To date, close to 30 MXenes (including $Ti_3C_2T_x$, Ti_2CT_x,[18] $Nb_4C_3T_x$,[19] Ti_3CNT_x,[20] $Ta_4C_3T_x$,[21] Nb_2CT_x,[22] V_2CT_x,[23] and $Nb_4C_3T_x$)[24] have been successfully introduced. Among these titanium-based MXenes, Ti_2CT_x is the most compatible for environmental applications due to its non-toxic nature and high abundance. In particular, $Ti_3C_2T_x$ is the most extensively studied in the category of MXenes.[25] Moreover, two or more transition metals have been established in MXene composition and can have ordered or disordered structures (*e.g.*, $Mo_2Ti_2C_3$,[26] $(V_{0.5}, Cr_{0.5})_3C_2$, and $(Ti_{0.5}, Nb_{0.5})_2C$).[26,27] Additionally, MXenes containing nitrides and carbonitrides have been examined in a few reports related to electrochemical energy storage and biological applications.[28,29] However, except for titanium carbonitride (Ti_3CN), it is difficult to synthesize nitride MXenes using selective acid etch procedures, and this is a limiting factor for the extensive investigation of nitride and carbonitride MXenes in pollutant removal applications.[30]

MXenes have been extensively researched for environmental applications since their discovery in 2011. Early research (2013)

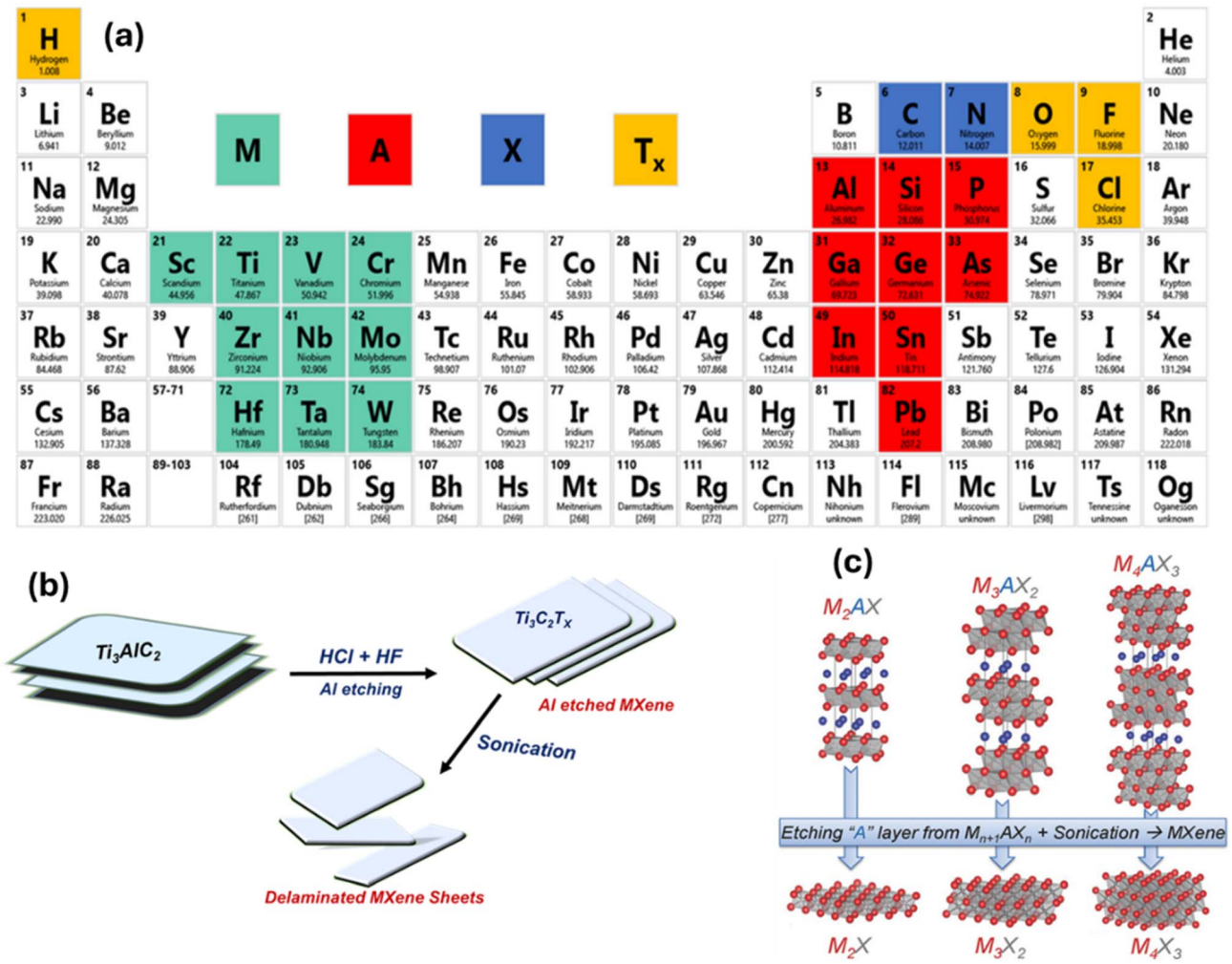

Fig. 1 (a) Elements used in MXene synthesis. Reprinted from ref. 31 with permission from the American Chemical Society, *Chem. Mater.*, Copyright 2018. (b) Schematic of the exfoliation process in the synthesis of $Ti_3C_2T_x$ MXenes from the max phase. (c) Exfoliation process for Ti_3AlC_2. Reprinted from ref. 53 with permission from Wiley, *Adv. Mater.*, Copyright 2014.

studies focused on heavy metal adsorption, while later studies focused on developments in photocatalysis for pollutant degradation (2017) and water filtering (2019). Mxenes are attractive components for environmentally friendly remediation technologies because of their remarkable conductivity, hydrophilicity, and chemical stability.[31] Two-dimensional (2D) nanomaterials exhibit confinement in the thickness dimension at the atomic scale, while their lateral dimensions range from tens of nanometres to several micrometres. Such properties of MXenes permit their use in many processes, like designing devices, spray coating, painting, and filtration.[32] In addition, Mxene polymer and Mxene graphene composites have been made to enhance the performance of the unaltered components, which include the creation of conductive channels and enhancing its overall stability.[33,34]

Pristine MXenes and Mxene-based materials have a massive effect in the fields of energy conservation and biological applications.[35,36] Other emerging applications include electrocatalysis, photocatalysis,[37] reinforcement for composite materials,[38] electromagnetic interference shielding,[39] gas and biosensors,[40–42] and transparent conducting electrodes.[43] As described, MXenes are synthesized from environment-friendly and abundant elements like C, Ti, and N. Hence, their environmental degradation results in nontoxic byproducts like CO_2 gas, N_2 gas, and Ti. Accordingly, MXenes are very suitable for applications related to environmental remediation.

This review article is centered on MXenes and Mxene-based composite materials for aqueous media application, which includes remediation of pollutants like heavy metals,[44,45] dyes,[46] and radionuclides,[47] organic contaminants,[48] and in water purification membranes.[49] This review uniquely consolidates the current knowledge on MXenes and Mxene-based materials for the removal of emerging water contaminants, including heavy metals, dyes, PFAS, pharmaceuticals, and micro-/nanoplastics. Unlike previous reviews, it critically evaluates the underlying removal mechanisms, material regeneration strategies, and potential environmental and health risks associated with MXenes and their degradation products. This review highlights gaps in the large-scale production, toxicity assessments, and the development of robust, recyclable Mxene-based membranes, providing a roadmap for future research. By integrating synthesis approaches, functional modifications, and application-specific performance, this work aims to guide the design of sustainable, next-generation water remediation technologies.

2 Different techniques for the synthesis of MXenes

2.1 Direct acid etching method

MXenes are synthesized by selectively etching the "A" group element, where A is silicon or aluminum (Al), from their respective MAX phase precursors at room temperature.[50,51] The MAX phase most frequently used as a starting reactant for synthesizing $Ti_3C_2T_x$ is Ti_3AlC_2. In this method, Al layers are removed from Ti_3AlC_2 using HF as the etchant. The MAX powder is stirred in HF for several hours, after which the mixture is washed with deionized water and centrifuged until the pH reaches 4–6.[52,53] During etching, Al nanolayers are replaced by terminal T_x groups (–OH, =O, and –F), as shown in Fig. 1b. Subsequent ultrasonic delamination yields graphite-like thin sheet structures (Fig. 1c), comprising single or a few layers of MXenes. MXenes prepared *via* HF etching can be sensitive to highly acidic conditions, potentially leading to aggregation or partial degradation. Washing and neutralization after etching help stabilize the sheets, while mild acidic to neutral pH conditions generally preserve the structural integrity. Surface functionalization or embedding into polymeric/ceramic matrices can further enhance the stability in more acidic environments. The quality of MXenes depends on factors such as the temperature, particle size of the MAX phase, HF concentration, and etching time.[54]

2.2 *In situ* acid etching method

Recently, numerous attempts have been made to replace the hazardous HF and other fluoride-based salts by adopting a process that utilizes lithium fluoride (LiF) and hydrochloric acid (HCl) instead of HF. In this method, HF is formed *in situ*. This method enhances MXene dispersion and biocompatibility, while having a minimal impact on the environment.[55,56] Li ions increase the expansion of the interlayer space once the procedure starts with the controlled loosening of the interlayer van der Waals bonds inside the MXene frameworks. The capacity to precisely modify MXene features like thickness, surface adaptability, and intercalation is one of the main advantages of *in situ* etching. In water treatment operations, the regulation of the interlayer gap expansion improves accessibility to active sites within layers, hence fostering effective interconnections with targeted molecules or ions. Additionally, the introduction of specific functional groups such as hydroxyl (–OH), carboxyl (–COOH), and amino ($–NH_2$) through *in situ* etching enhances MXene's water treatment properties. These functional groups improve surface wettability, selectively adsorb impurities, and facilitate specific chemical reactions, making MXenes produced by *in situ* etching highly suitable for pollutant removal and water purification applications. A lower reaction rate during HF etching is particularly advantageous, as it allows for a more controlled removal of the A layers from MAX phases, preserving the 2D layered structure and surface terminations. This control yields MXenes with more uniform morphology, higher surface area, and enhanced active sites, which are critical for adsorption and catalytic efficiency. Moreover, slower reactions reduce exothermic hazards and uncontrolled gas evolution, enabling safer, reproducible, and scalable production for practical water treatment applications. The possibility of further improving the MXene characteristics by adding additional chemicals and minimizing handling or transfer steps ensures maximal exposure of functional surfaces, further enhancing interactions with environmental pollutants. Different MXene synthesis pathways are shown in Fig. 2, together with the associated surface morphology, interlayer spacing, and surface functionality, as established by various optimization methods. The morphology

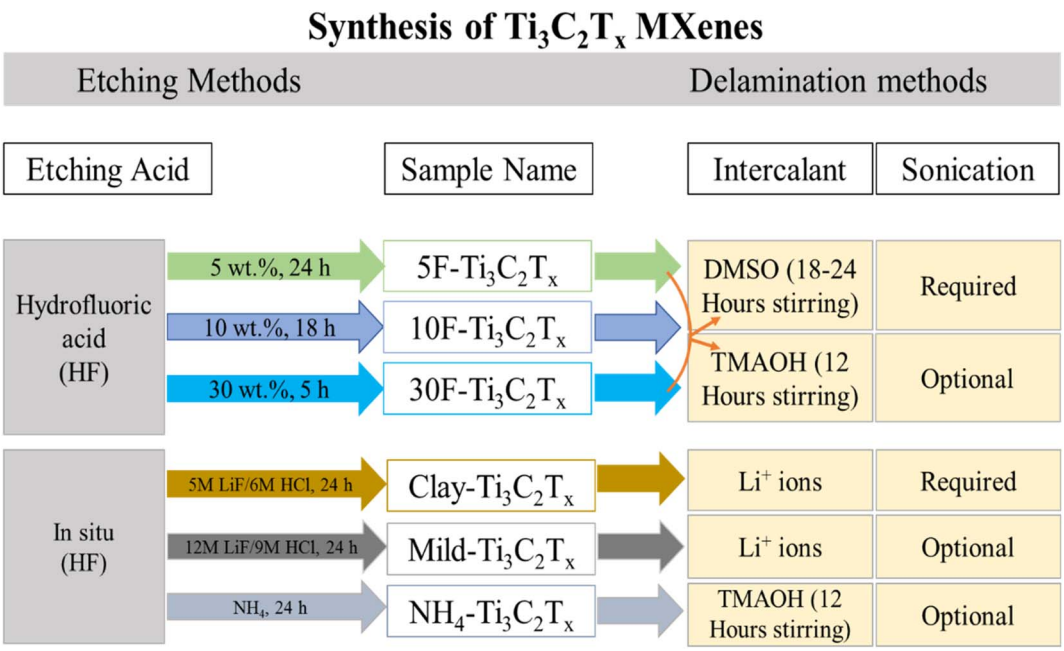

Fig. 2 Synthesis methods of delaminated MXenes utilizing direct HF and *in situ* HF techniques. Reprinted from ref. 52 with permission from the American Chemical Society, *Nano*, Copyright 2017.

of different MXenes visualized using scanning electron microscopy (SEM) is depicted in Fig. 3.

2.3 Other methods

Alkali etching and electrochemical etching are two feasible alternative techniques for the synthesis of MXenes without using fluorides. These methods improve the sustainability and adaptability of MXene fabrication methods by expanding the possibilities for MXene manufacturing and reducing concerns about the use of fluoride.[57] The top-down (i) hydrothermal, (ii) molten salt, and (iii) electrochemical etching approaches, as well as the bottom-up (iv) vapor deposition etching (CVD) and atomic layer deposition (ALD) routes for the synthesis of MXenes, are schematically represented in Fig. 4. A safe and efficient substitute for HF vapor in the preparation of MXenes is the hydrothermal approach.[58] In this process, $Ti_3C_2T_x$ is initially treated in an alkaline solution, which expands the interlayer spacing and introduces hydroxyl (–OH) groups on the MXene surface, improving hydrophilicity. The aluminum layer is then hydrothermally treated with sulfuric acid, which removes

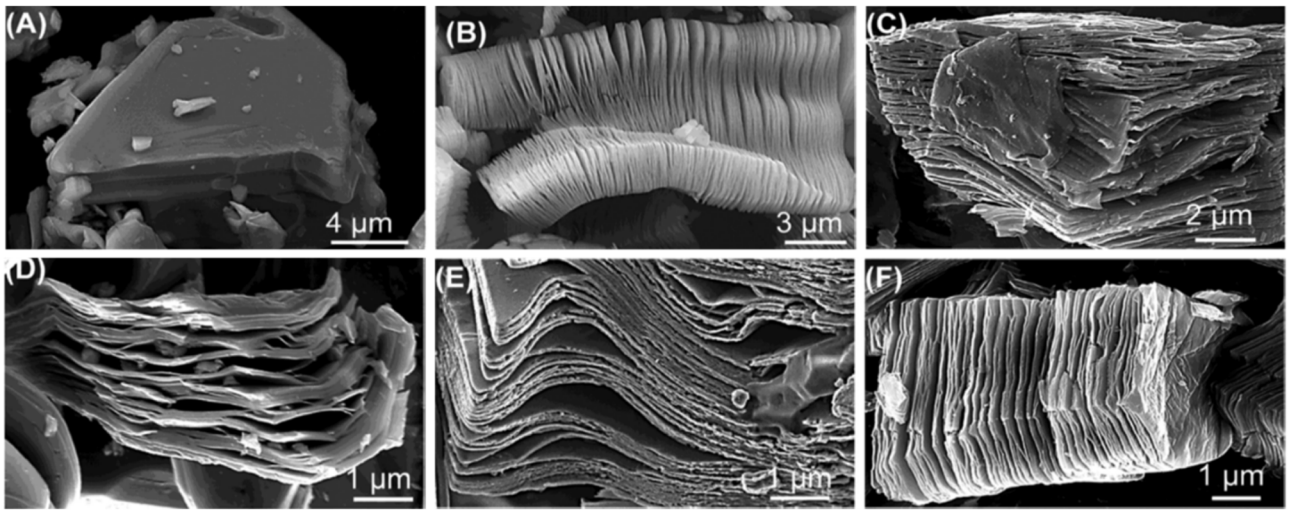

Fig. 3 SEM images for different MXenes: (A) and (B) Ti_3AlC_2 particle before and after ($Ti_3C_2T_x$) HF treatment, (C) Ti_2AlC after HF treatment, (D) Ta_4AlC_3 after HF treatment, (E) TiNbAlC after HF treatment, and (F) Ti_3AlCN after HF treatment. Reprinted from ref. 21 with permission from the American Chemical Society, *Nano*, Copyright 2012.

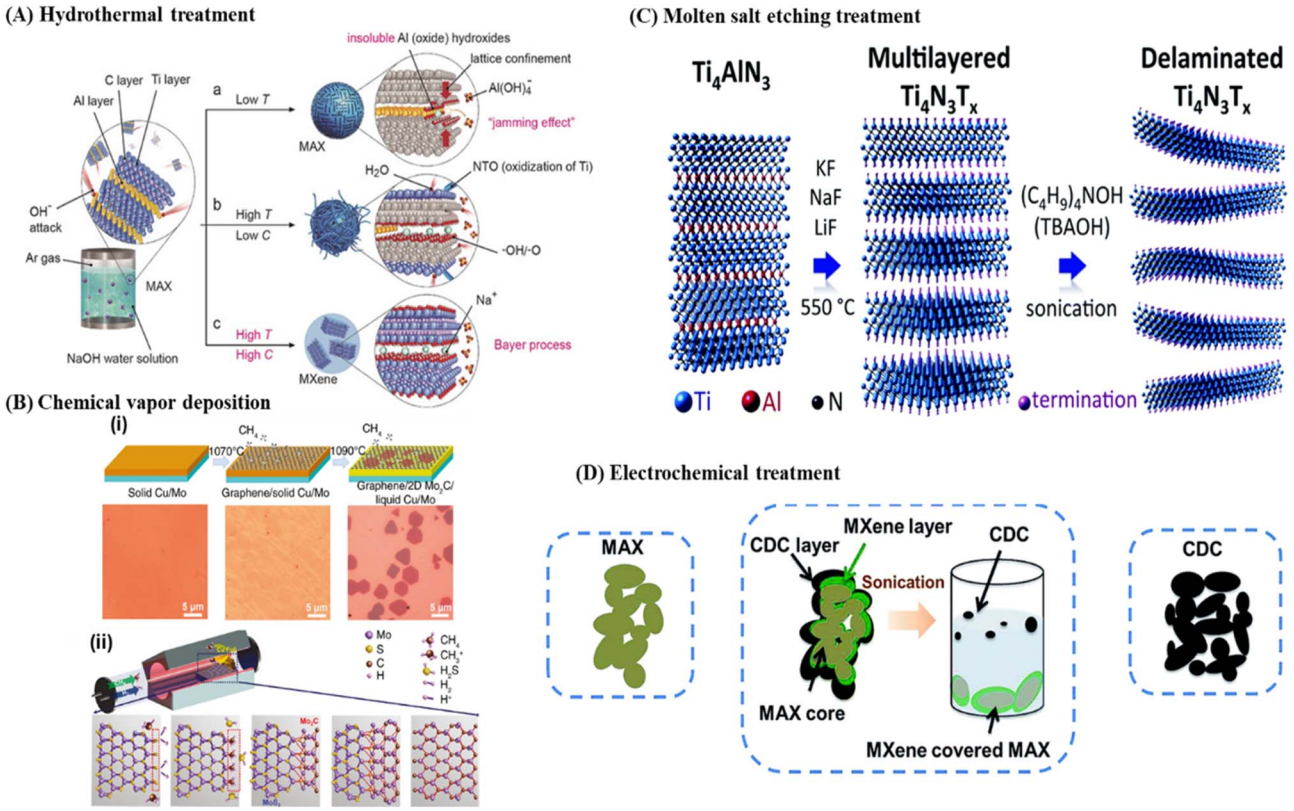

Fig. 4 Schematic of the top-down and bottom-up synthesis approaches for MXenes: (A) hydrothermal treatment, (B) CVD, (C) molten salt etching, and (D) electrochemical treatment. Reprinted from ref. 58 with permission from MDPI, *Molecules*, Copyright 2022.

residual metal species and partially protonates the surface, resulting in structurally stable and well-functionalized MXene sheets. This two-step hydrothermal method differs from dedicated alkali etching using NaOH, as it allows for a more controlled exfoliation, uniform surface functionalization, and enhanced dispersibility, all of which contribute to improved lattice characteristics, more complete aluminum removal, and superior pollutant adsorption capabilities. To create new MAX phases, element substitution in molten salts has also been employed.[59,60] To avoid the hazards associated with HF vapor, a hydrothermal method has been developed as a safer and more efficient pathway for MXene synthesis.[61,62] Utilizing inorganic alkalis like NaOH, the alkali etching technique removes aluminum from its initial MAX phase.[63] For example, an alkali-assisted hydrothermal etching method was used to create titanium carbide MXenes with a purity of 92% by weight.[64] In order to stop oxidation, the MAX phase is treated in an argon environment while in an aqueous solution of NaOH. It is beneficial to dissolve aluminum hydroxides and oxides at higher alkali concentrations and temperatures. Electrochemical etching is another fluoride-free technique that isolates certain nanolaminate components, like carbon produced from carbide.[63] This strategy minimizes the etchants' negative effects by decreasing the reliance on them for MXene synthesis. Because there are no fluorine-based etchants or only a small amount of them, the resulting exfoliated MXenes are fluorine-free. High-quality, flawless 2D MXenes can be produced using the bottom-up technique, including atomic layer deposition ALD and CVD.[63] Electrochemical etching is another fluoride-free technique that specifically removes the nanolaminate. When creating 2D sheets from metal carbides, these fluorine-free methods provide versatility in terms of the number of layers. This technique is safe for the environment and can prepare MXenes like Mo_2C.[65] All things considered, these different approaches to synthesizing MXenes not only increase the compounds' potential and uses, but also solve the safety and environmental issues related to conventional fluoride-based etching techniques. Overall, fluoride-free synthesis routes—such as alkali etching, hydrothermal processing, molten-salt methods, electrochemical etching, and bottom-up ALD/CVD growth—offer safer and more sustainable alternatives to conventional HF-based MXene fabrication. These methods enable effective A-layer removal, improved structural control, and the production of fluorine-free or high-purity MXenes that are suitable for environmental applications. Together, they expand the versatility of MXene synthesis, while addressing major safety and environmental concerns.

3 MXenes for water purification

There is increasing interest in exploring MXenes and its derivatives in water treatment because of its remarkable properties. MXenes also possess extraordinary reductive, antibacterial, and adsorptive properties, high hydrophilicity, and electronic

conductivity. As MXenes show generous sorption selectivity and reduction capability, it can be used in many water purification techniques. Generally, $Ti_3C_2T_x$ and related composites are widely used in water treatment for removing heavy metals, radionuclides, and dyes. In water treatment, adsorption is mainly used for the remediation of pollutants because of the benefits of easy operation, low cost, regeneration capability of adsorbents, less sample destruction, and abundant availability of adsorbents.[66,67] Different nanomaterials, including carbon nanotubes,[68] graphene-based materials,[69] metal oxides,[70] and dendrimers,[71] are broadly used as adsorbents for the remediation of water pollutants. MXenes have been successfully utilized in capacitive deionization (CDI), membranes, and photocatalysts, as well as in electrosorption and adsorption-based platforms for water purification. Their high surface area, tunable interlayer spacing, and abundant surface functional groups enable the efficient capture of ions, heavy metals, dyes, and other contaminants, highlighting their versatility as both functional components in devices and standalone adsorptive materials.[72–76]

3.1 Remediation of heavy metals and radionuclides *via* MXene adsorbents

Chemical industries have contributed significantly to heavy metal pollution in ecosystems.[77] Heavy metals generally have atomic weights ranging from 63 to 201 and a density of more than 5 g cm^{-3}.[78] They accumulate in living organisms, as most heavy metals are not biodegradable.[79] The contamination of water bodies with heavy metals (*e.g.*, zinc, mercury, nickel, copper, cadmium, lead, and chromium) disrupts aquatic ecosystems and constitutes a pressing global environmental issue.[80,81] MXenes have demonstrated potential in the remediation of heavy metals *via* adsorption.[82] The interlayer separation (<2 Å) in MXenes plays an essential role as the heavy metal ions (<4.5 Å) are confined between these voids. Furthermore, the surface functional groups of MXenes are responsible for enhancing efficient adsorption capability. Popularly, titanium-based MXenes ($Ti_3C_2T_x$) have been used to effectively adsorb different concentrations of metal ions.[45,83–85] Fard *et al.* reported on the preparation of $Ti_3C_2T_x$ nanosheets using the exfoliation method.[86] These nanosheets were used to adsorb Ba(II) ions from aqueous solutions with better uptake capacity. Approximately 90% of ions were adsorbed within 10 min by $Ti_3C_2T_x$ nanosheets. By keeping the Ba(II) ion dosage at 100 mg and using a starting concentration of 55 ppm, the adsorption capacity of $Ti_3C_2T_x$ was observed to be 9.3 mg g^{-1}. The presence of other counterions did not interfere much with the adsorption process, which involves both physisorption (on the MXene's surface) and chemisorption (because of the functionalities present on the MXene's surface). This led to the sorption of Ba(II) ions on the $Ti_3C_2T_x$ nanosheets. Xiaofang Feng *et al.* experimented with titanium carbide as a 2D adsorbent alk-MXene/LDH (layer double hydroxide) to remediate Ni^{2+}.[87] Owing to its distinctive sheet-like structure, the functional groups and desirable binding sites of alk-MXene/LDH provide a superior adsorbent for eliminating these ions in aqueous media. The sorption capability of the adsorbent was 222.7 mg g^{-1} for Ni^{2+}. The efficiency of the removal of Ni^{2+} was 97.35% at a wide range of pH environments (from 5 to 13), as shown in Fig. 5. This adsorbent exhibits excellent reproducibility after eight successive adsorption–desorption cycles. Xuefeng Sha *et al.* reported on the synthesis of MXenes-based bismuth oxide (MXenes-PDA Bi_6O_7) through mussel-inspired chemistry that is based on the formation of dopamine to form polydopamine (PDA) layers *via* self-polymerization on MXenes for the successful confinement of Bi_6O_7 particles.[88] This composite was used to eliminate iodide ions by the sorption phenomenon. The sorption capacity was 64.65 mg g^{-1}, which is higher than that of pristine MXenes under the same experimental conditions. Defu Gana *et al.* reported on MXenes-related polymeric nanocomposites ($Ti_3C_2T_x$-PDOPA).[89] The resultant $Ti_3C_2T_x$-PDOPA composites were utilized as an efficient adsorbent for the remediation of Cu^{2+}, exhibiting a sufficient sorption capacity of 65.13 mg g^{-1}, compared to raw MXenes.

Lelin Hea *et al.*[90] used zero-valent iron particles to prepare nanocomposite MXenes. To investigate the removal of Cr(VI), a nanoscale component was introduced into the interlayer spacing of alkaline-intercalated Ti_3C_2 (alk-Ti_3C_2). The absorption capacity of Cr(VI) (194.87 mg g^{-1} at pH = 2) may be enhanced by the longer interlayer space of alk-Ti_3C_2 and the increased active sites of nZVI. Even with the presence of other coexisting cations, the extremely effective removal of Cr(VI) was maintained, demonstrating significant promise for actual environmental cleanup. The mechanistic analysis revealed that the synergistic impacts of the two nanosheets are the key to removing Cr(VI) from nZVI-alk-Ti_3C_2 composites. Shahzad *et al.* synthesized a highly magnetic titanium carbide ($Ti_3C_2T_x$) MXene composite (MGMX) through a simple hydrothermal method, and used it for the elimination of mercuric ions (Hg(II)) in the aqueous phase *via* adsorption.[91] The MGMX nanocomposite demonstrated excellent removal of Hg(II) under various pH conditions. A remarkable adsorption capacity was observed, *i.e.*, 1128.41 mg g^{-1} for Hg(II). Faisal *et al.* synthesized a δ-MnO_2/MXene *in situ* hybrid (IH) composite using the hydrothermal method for the remediation of Cr(VI) *via* the adsorption process at various pH values.[92] The highest obtained sorption capacity was 353.87 mg g^{-1}. Yongjun Tian *et al.*[73] prepared 2D alk-MXene ($Ti_3C_2(OH/ONa)_xF_{2-x}$) for the large-scale adsorption of Pb(II). The layered structure of this MXene composite exhibits a highly active site (Ti–OH), which subsequently offers significant potential in the remediation of Pb(II) from aqueous media. The high adsorption capacity of 140 mg g^{-1} is achieved even with other ions like Ca(II)/Mg(II) in high amounts. The adsorption equilibrium is attained quickly in a time period of only 120 seconds.

Nuclear power plays an essential role as traditional fossil fuel resources are getting depleted. It is considered to be carbon-free as it does not emit any greenhouse gases; however, radionuclides (having high mobility and long half-lives) like uranium (235 and 238), thorium (232), barium (133, 140), cesium (137), and strontium (90) are being liberated into the environment due to the substantial utilization of nuclear energy and operation of nuclear powerplants.[93] The rapid growth of industries

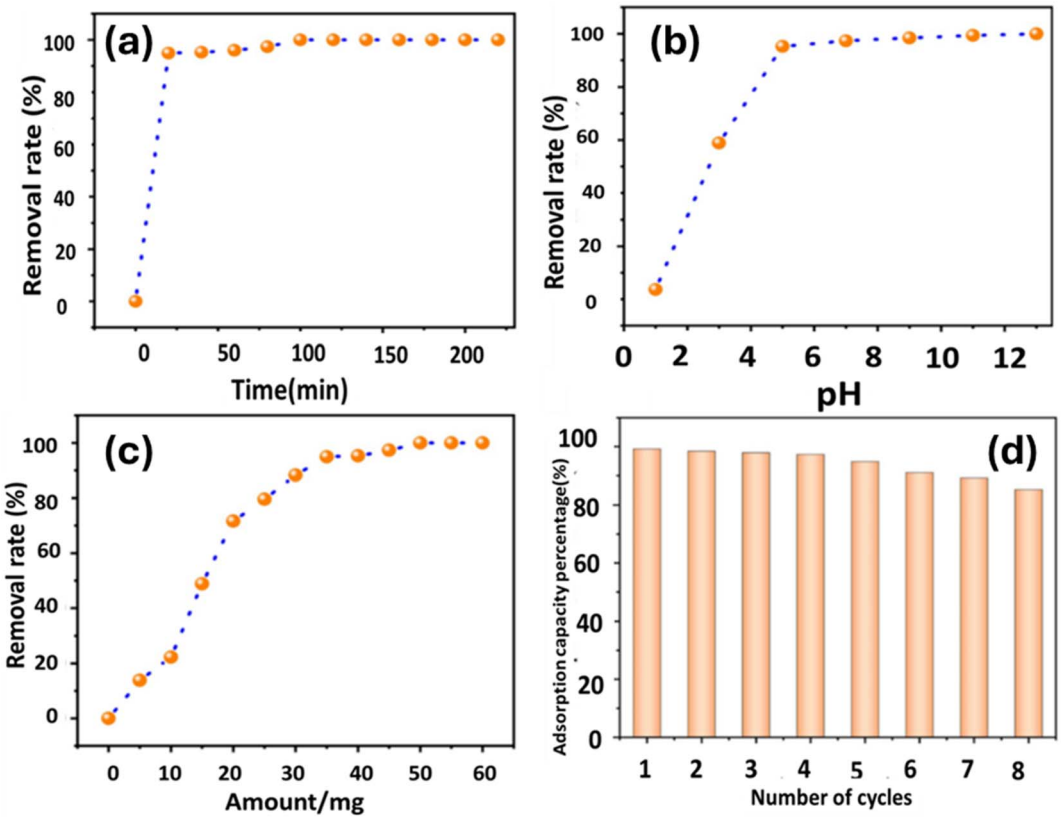

Fig. 5 (a–c) Effect of adsorbent (MXenes-LDH) amount, contact time, and pH on Ni^{+} adsorption. (d) Reusability of MXenes-LDH. Reprinted from ref. 87 with permission from Elsevier, *Sep. Purif. Technol.*, Copyright 2020.

related to nuclear power has resulted in environmental pollution because of the emission of nuclear waste. This critical situation has gained significant attention as it is associated with adverse environmental effects.[94] Adsorption is the most common and effective technique for the remediation of contaminants from nuclear debris, among other techniques.

MXenes have distinct qualities and have emerged as cutting-edge adsorbents for the remediation of different radionuclides like uranium, palladium, europium, cesium, and thorium.[95–102] Hydroxylated vanadium carbide MXene ($V_2C(OH)_2$) nanosheets have conclusively shown the elimination of uranium ions $[UO_2(H_2O)_n]^{2+}$ experimentally and theoretically as well. According to the experimental procedure, MXene $V_2C(OH)_2$ provides a high sorption capacity (*i.e.*, 174 mg g^{-1}) for uranium.[98,99] Furthermore, MXenes remove polluted water from radionuclides like cesium ions (Cs^{+}). MXenes like $Ti_3C_2T_x$ have shown a sorption capability of 25.4 mg g^{-1} and attained equilibrium within sixty seconds. The removal efficiency is quite effective for up to 5 cycles, as shown in Fig. 6.[100] The sorption capacity is high due to the existence of functional groups (*i.e.*, fluorine groups, oxygen, and hydroxyl) and the structure of MXenes. Other studies have recorded an adsorption capacity of 148 mg g^{-1} for Cs^{+} by MXenes ($Ti_3C_2T_x$).[101] Another study showed the remediation of Cs^{+} from wastewater utilizing composite nanomaterials. Asif Shahzad *et al.*[101] synthesized titanium-based MXenes integrated with Prussian blue aerogel spheres (PBMX sphere). These spherical structures have high porosity and unique structures with enriched oxygen-containing functional groups. The PBMX sphere effectively removes Cs^{+} from wastewater under all conditions, including neutral, acidic (1 M HCl), and basic (pH 11) conditions. These nanocomposites have a sorption capacity of 315.91 mg g^{-1} for Cs^{+}, the highest value reported for such identical adsorbents. Another study reported the removal of Ba^{2+} and strontium (Sr^{2+}) by $Ti_3C_2T_x$ from wastewater. Electrostatic attraction, ion exchange, and inner-sphere complex production are responsible for the adsorption of Ba^{2+} and Sr^{2+} at different pH values onto the MXenes when other ions are also present in the media (like NaCl and $CaCl_2$).[74] The adsorption capacity exhibited by the MXenes was excellent (180 mg g^{-1} and 225 mg g^{-1} for Ba^{2+} and Sr^{2+}, respectively). Moreover, the MXenes could be reused for up to four cycles. High sorption capacity and selectivity for the adsorption of thorium Th(IV) ions were demonstrated by the hydrated MXenes compared to its dry counterpart.[18] Hydrothermal oxidation and alkalization techniques for the synthesis of MXenes were used to prepare hierarchical titanate nanostructures (HTNs). Fig. 7 shows the efficient uptake of Eu(III) ions by the MXenes-based nanostructures (HTNs) with excellent adsorption capacities (more than 200 mg g^{-1}). Immobilization was demonstrated by the exchanged Eu(III) ions, as the ions were restricted in the layers of the MXenes.[93] MXenes effectively adsorbed Pd(II) with a high sorption capacity of 184.56 mg g^{-1}.[103] A reported study

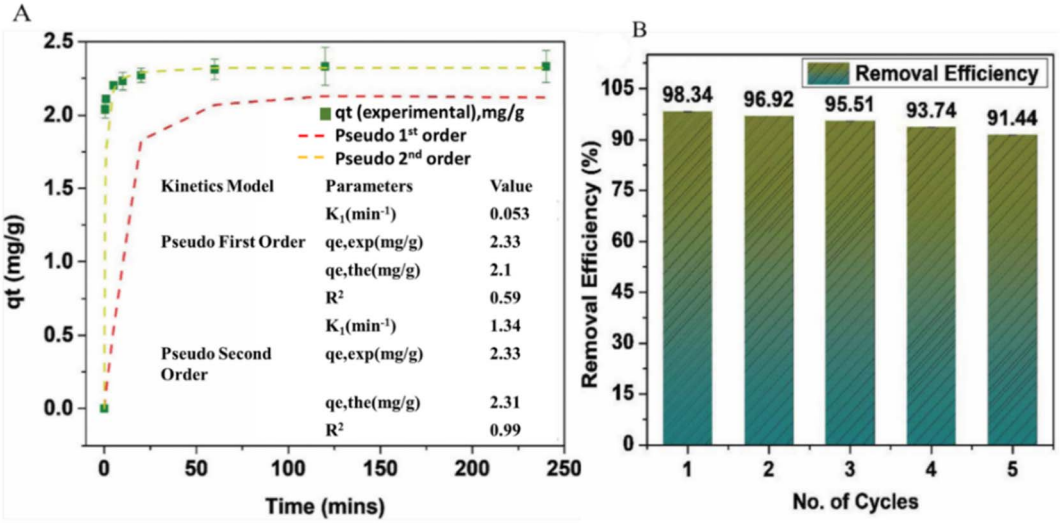

Fig. 6 (A) Effect of competitive ions on Cs^+ adsorption. (B) Reusability of $Ti_3C_2T_x$ for Cs^+ adsorption. Reprinted from ref. 100 with permission from the Royal Society of Chemistry, *Dalton Trans.*, Copyright 2019.

showed the experimental sorption capacity of 160 mg g^{-1} of uranium U(IV) using a hydration intercalation process that includes DMSO.[104] Intercalated $Ti_3C_2T_x$ shows an adsorption capacity that is five times higher than that for the dry $Ti_3C_2T_x$. The interlayer space has a major impact on U(IV) adsorption, as the enlargement of the interlayer space can directly enhance the adsorption phenomenon. Some reports have observed the adsorption of U(VI) *via* reduction of U(VI) to U(IV). The observed sorption capacity was 470 mg g^{-1}.[95] Zhao *et al.* synthesized a porous structured MXene gel initiated *via* calcium ions (3D MXene-Ca) for the adsorption of U(VI) ions in water with the highest sorption capacity of 823.6 mg g^{-1}.[105] Shi *et al.* synthesized iron nanoparticles on alkaline MXene nanoflakes (nZVI/alk$Ti_3C_2T_x$) by an *in situ* growth method for the removal and

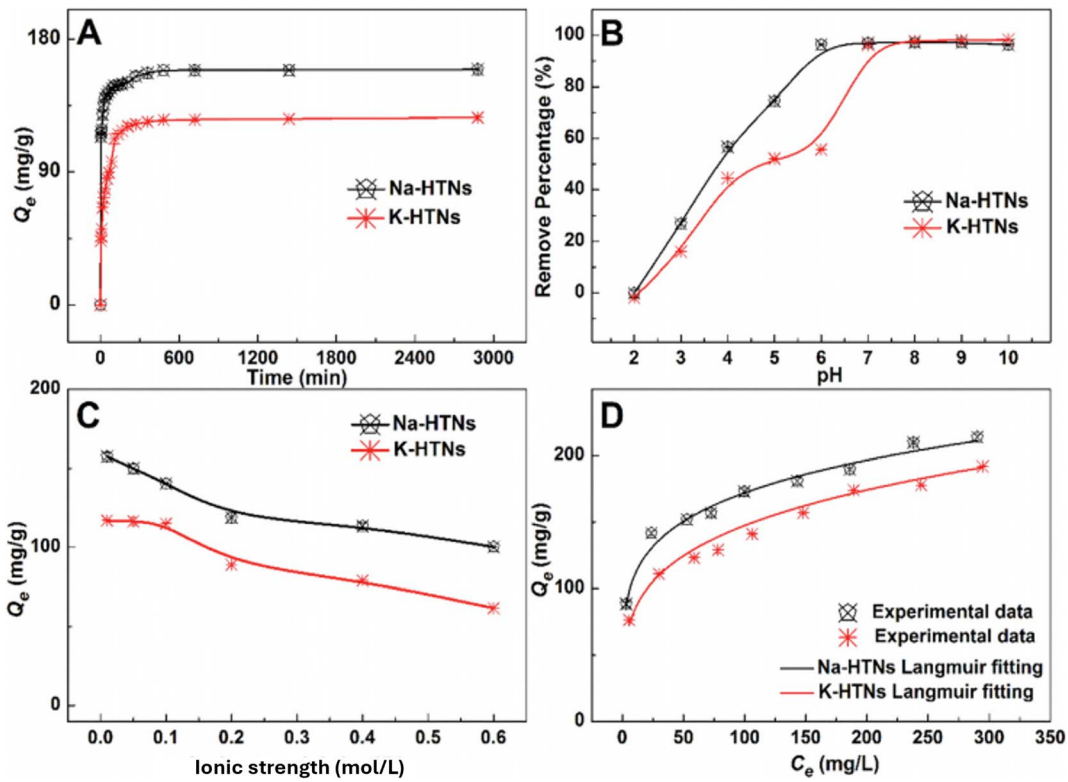

Fig. 7 Eu(III) removal by MXene-based Na-HTNs and K-HTNs as a function of (A) contact time, (B) pH, (C) ionic strength, and (D) equilibrium concentration. Reprinted from ref. 93 with permission from the Royal Society of Chemistry, *Environ. Sci.: Nano*, Copyright 2020.

reduction of U(VI) from the water with an adsorption capability of 1315 mg g^{-1}.[106] MXenes and their composites are highly effective adsorbents for water purification due to their high surface functionality, tunable interlayer spacing, and strong reductive/adsorptive properties. They efficiently remove heavy metals (*e.g.*, Pb^{2+}, Hg^{2+}, and Cr(VI)) and radionuclides (*e.g.*, U, Cs, Sr, and Eu) with fast kinetics, high capacity, and excellent reusability. MXene-based composites further enhance adsorption through synergistic effects, structural expansion, and additional active sites, making them promising candidates for practical and scalable water treatment applications.

3.2 Removal/degradation of dyes *via* MXene adsorbents

Dye pollution hazards have significantly increased in recent years as dyes are one of the most consumed chemicals in the textile industry. The consumption is about ten thousand tonnes annually, out of which approximately 100 tonnes are discharged into wastewater.[107] The adsorption method is one of the most promising approaches to remove dyes as it is a fast, safe, low cost, and efficient method.[108,109] Materials related to MXenes have shown excellent potential for the elimination of dyes.[110] Many dyes, including methyl orange (MO),[111] methyl blue (MB),[112] rhodamine B (RhB),[113] neutral red (NR),[114] acid blue 80 (AB80),[112] and safranine T (ST),[114,115] were remediated by MXenes and MXene-based nanomaterials. Reports have also shown enhanced degradation when the adsorption was performed under illumination with UV light. Adsorption of MB was performed by Zheng Wei *et al.*[116] using different hot alkaline-treated MXenes like NaOH–$Ti_3C_2T_x$, LiOH–$Ti_3C_2T_x$, and KOH–$Ti_3C_2T_x$. Out of these different MXenes, NaOH–$Ti_3C_2T_x$ showed an outstanding sorption capacity of 189 mg g^{-1} for MB. A 29% expansion in the interlayer was observed with LiOH by altering the surface functionality. The surface area enhancement increased the efficiency and capacity uptake of NaOH–$Ti_3C_2T_x$ in comparison to those of the pristine MXenes, as shown in Fig. 8. The etching method for producing MXenes is a crucial factor in enhancing the adsorption of dyes. Ti_3C_2 is prepared using both hydrothermal and HF etching methods. The adsorption observed for MB using MXenes prepared *via* the hydrothermal method was more rapid and efficient than that of the conventionally etched MXenes. In the case of MO, which was not practically adsorbed by MXenes prepared by either hydrothermal or HF etching methods,111 this limitation is attributed to weak electrostatic interactions and the absence of suitable active sites for anionic dye capture. To overcome such inherent limitations, Chong Cai *et al.*[117] synthesized a MXene-based phytic acid (PA–MXene) composite *via* a hydrothermal process, achieving significantly improved dye removal. In comparison to the pristine MXenes, the PA–MXene composite exhibited enhanced sorption characteristics toward dyes such as MB and RhB, with its sorption capacity for MB remaining at approximately 85% after 12 cycles, demonstrating strong durability for wastewater applications. Yi Cui *etal.*[118] further advanced this concept by creating magnetic MXene composites (Ti_3C_2-MNPs) through a one-pot method, in which thermal treatment anchored ~5 nm Fe_3O_4 nanoparticles uniformly onto the Ti_3C_2 sheets. While pristine $Ti_3C_2T_x$ shows poor affinity for MO, the incorporation of Fe_3O_4 nanoparticles introduces new catalytic active sites and facilitates electron-transfer pathways, enabling the rapidly advanced oxidation of MO and other dyes. As shown in Fig. 9, these Ti_3C_2-MNPs composites can catalytically degrade RhB, MO, MB, and Congo red (CR) through synergistic adsorption-catalysis mechanisms, illustrating how surface modification transforms MXenes from weak MO adsorbents into highly effective catalytic platforms. Free radicals, such as OH and O_2^-, are essential to the degradation process. For RB, MO, CR, and MB, the absolute degradation times were 7 min, 12 min, 7 min, and 6 min, respectively. The catalytic degradation results illustrated that Ti_3C_2-MNPs had high degradation efficiency toward these organic dyes. Ti_3C_2-MNPs maintained satisfying performance after cyclic use, indicating that Ti_3C_2-MNPs are a favorable contender for adsorption. Yuan *et al.*[119] synthesized an efficient adsorbent (Ti_3C_2–SO_3H) using sulfanilic acid for modification of the surface. The above adsorbent can remove MB from the aqueous media. The results showed an efficient sorption capacity of 111.11 mg g^{-1} in comparison to that for raw MXene (21.10 mg g^{-1}). Surface functionalization with sulfanilic groups was found

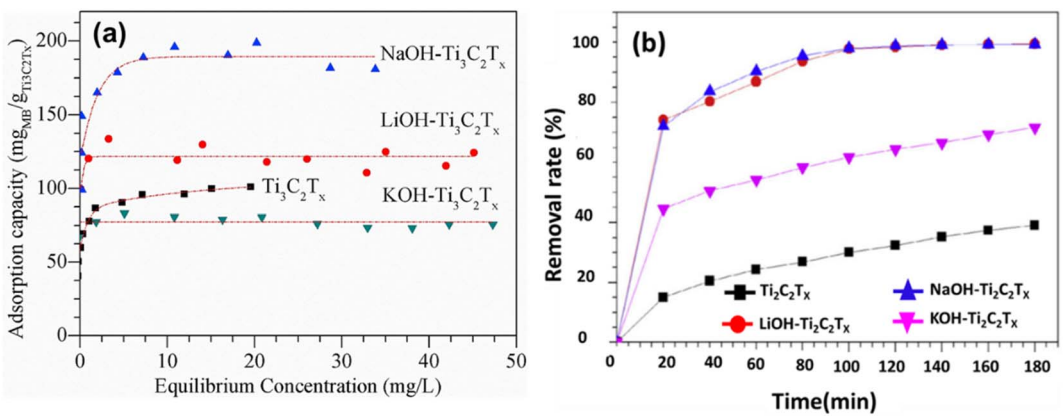

Fig. 8 (a) Plot of the MB removal rate *vs.* time for different absorbents. (b) Adsorption isotherms of MB on $Ti_3C_2T_x$, LiOH–$Ti_3C_2T_x$, NaOH–$Ti_3C_2T_x$, and KOH–$Ti_3C_2T_x$. Reprinted from ref. 116 with permission from Elsevier, *Mater. Chem. Phys.*, Copyright 2018.

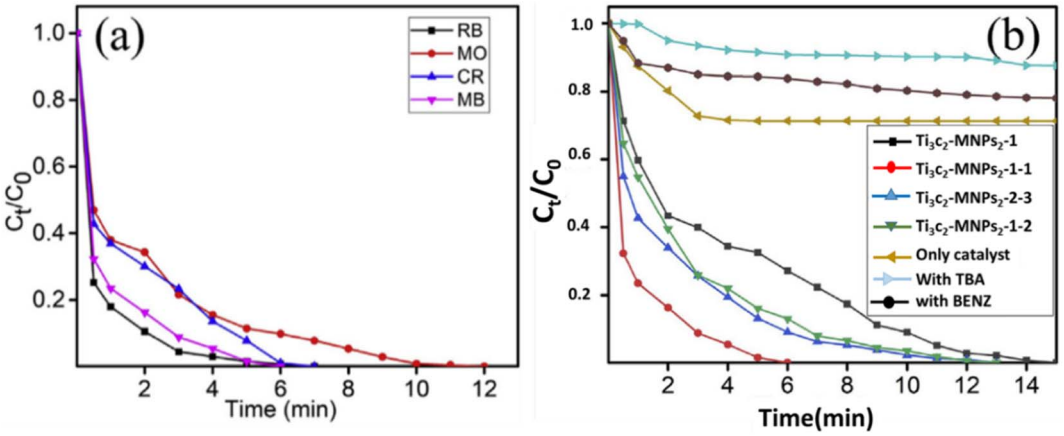

Fig. 9 (a) Degradation efficiencies of Ti_3C_2-MNPs on four organic dyes. (b) Degradation efficiencies of Ti_3C_2-MNPs with different mass ratios. Reprinted from ref. 95 with permission from the American Chemical Society, *Environ. Sci. Technol.*, Copyright 2018.

to be beneficial in improving the uptake capacity of Ti_3C_2 for the adsorption of MB, owing to the electrostatic interaction between the adsorbent and cationic dye in an alkaline surrounding.

The adsorption efficiency can be increased by incorporating nanomaterials on the MXene surface. Byung *et al.*[120] incorporated a metal–organic framework (MOF) on the MXene surface and enhanced the adsorption capacity. These MXenes were used to adsorb MB and AB80. The surface areas recorded for the MXenes and MOF were 9 m^2 g^{-1} and 630 m^2 g^{-1}, respectively. These MXene composites showed excellent performance and attained a sorption capacity of 140 mg g^{-1} for MB and 200 mg g^{-1} for AB80. MOF can capture MB due to electrostatic interactions. The studies also defined the high selectivity of MXenes and the high adsorption capacity of MOF. MXenes and MXene-based composites are highly effective for the removal and degradation of dyes from wastewater due to their large surface area, tunable interlayer spacing, and abundant functional groups. Surface modifications and hybridization with materials like MOFs, phytic acid, or magnetic nanoparticles significantly enhance the adsorption capacity and degradation efficiency, while maintaining reusability over multiple cycles. These properties make MXenes promising candidates for rapid, selective, and sustainable dye remediation in water treatment applications.

3.3 Remediation of per-and poly-fluoroalkyl substances (PFAS) (emerging contaminant)

Per- and polyfluoroalkyl substances, or PFAS, represent a class of organofluorine compounds from anthropogenic sources. These synthetic chemicals comprise a polar head group and a non-polar tail, with fluorine–carbon (F–C) bonds, which make them difficult to break down.[121,122] Due to their unique structure, PFAS are remarkably chemically and thermally stable, which makes them popular in a broad range of products and applications. Although PFAS are used in specific applications like military operations, water-resistant clothing, and stain-resistant coatings, their primary use has been in household product manufacturing, such as nonstick cookware.[123,124] The growing use of PFAS has caused them to be easily released into ecosystems, where they accumulate, leading to the contamination of water systems. Furthermore, clear evidence shows that human exposure to PFAS can lead to hormonal imbalances, weakened immune function, weight gain, higher cholesterol levels, and an increased risk of cancer.[125] Recent reports have highlighted the concentration of PFAS in the body and its toxic properties.[126] Despite efforts to phase them out, PFAS have been detected throughout the 50 states in the US. Moreover, PFAS have been identified in numerous environments and 97% of analyzed human blood samples, underscoring their pervasive presence.[121]

MXenes exhibit excellent physicochemical properties, making them outstanding materials for the removal of PFAS from wastewater systems. Moreover, it can be used in various configurations and forms, such as an addition to hollow fiber membranes, as demonstrated by Le *et al.*[121] Scientists used a modified MXene thin-film nanocomposite, which is the base of the MXene-polyamide selective layer. The materials were prepared through an interfacial polymerization method that includes trimethyl chloride, along with a combination of piperazine and MXene nanosheets (see Fig. 10a). The presence of MXene allowed for tuning the selective layer's morphology and negative surface charge, enabling a 96% PFAS removal efficiency. Additionally, MXenes increased the water permeability by providing various mechanisms of transport for ions and PFAS particles, as well as influencing the physicochemical features of the PA layers, thereby optimizing the balance between permeability and rejection.

MXene-enhanced membranes are effectively used in electrosorption processes, which further enhance the efficiency of PFAS removal from water systems in electrocatalytic membranes. An example of this complex system is presented in the research by Ma *et al.*[127] Scientists utilized the superior electrical conductivity, adjustable surface properties, and large surface area of MXenes to remove perfluorocarboxylic acids (PFCAs), including perfluorobutanoic acid (PFBA) and

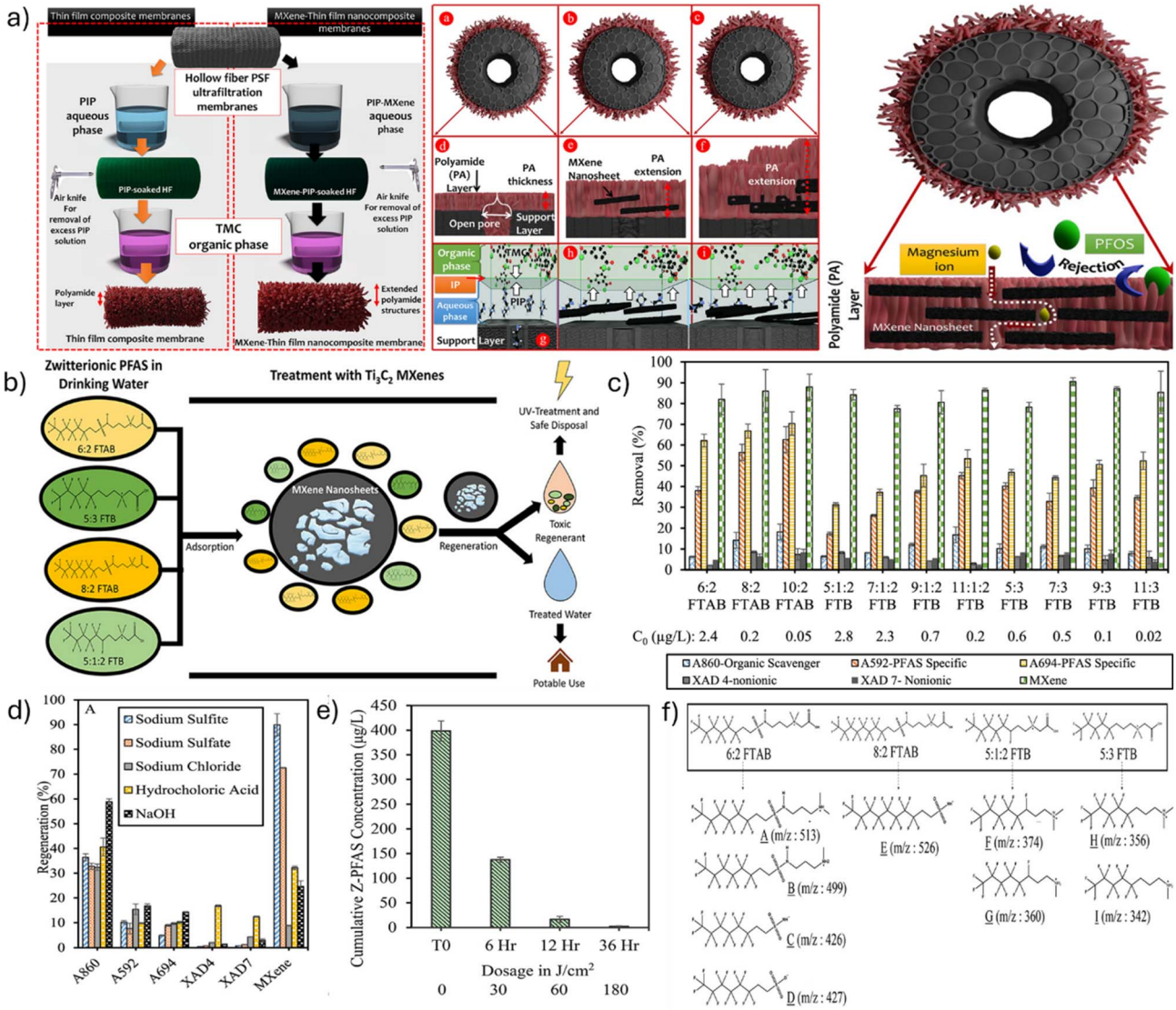

Fig. 10 (a) Production of fiber membranes through interfacial polymerization with MXenes, as a catalyst, and without them. Schematic of the hollow fiber and the process of removal of PFAS. Reprinted from ref. 121 with permission from the American Chemical Society, *Appl. Mater. Interfaces*, Copyright 2022. (b) Scheme of the process with the removal of PFAS with membranes containing MXenes. (c) Efficiency of different types of zwitterionic PFAS (fluorotelomer sulfonamidopropyl betaines and fluorotelomer betaines, known as FTAB and FTB, respectively) decomposition within the adsorbent media of three kinds of resins (typical, nonionic, and PFAS-specific), and Ti_3C_2 MXenes. (d) Efficiency of adsorbent regeneration. (e) Degradation of the summed zwitterionic PFAS, including FTAB and FTB, after 36 hours of UV/sulfite process. (f) Byproducts formed during the UV/sulfite process with FTAB and FTB solutions. Reprinted from ref. 123 with permission from American Chemical Society, *Environ. Sci. Technol.*, Copyright 2022.

perfluorooctanoic acid (PFOA). The PFAS rejection process involved three MXene variants, each terminating with oxygen, fluorine, or chlorine atoms, and analyzed their electrosorption, desorption, and oxidation characteristics. The study revealed that MXene with an –O functional group on its surface achieved an adsorption capacity of 215.9 mg g^{-1}, notably higher than MXenes containing –F and –Cl terminations. The same O-rich MXene also exhibited an oxidation rate constant of 3.9×10^{-2} min^{-1} for PFOA, and more than 99% of PFCAs were decomposed within 3 h under an applied potential of +6 V in 0.1 M Na_2SO_4. Interestingly, PFOA degraded more rapidly than PFBA by approximately 20%, highlighting the selective advantage of O-terminated surfaces. The electrosorption strategy was also explored by Shrestha *et al.*,[126] who enabled reversible PFAS adsorption–desorption cycles by integrating MXenes with poly(3,4-ethylene dioxythiophene) polystyrene sulfonate (PEDOT). These MXene-PEDOT membranes exhibited significantly increased surface area and pore volume, leading to a four-fold enhancement in the volumetric capacitance and stable cycling performance. A further advancement was demonstrated by Zhao *et al.*,[128] who introduced a highly porous polyaniline-MXene film that nearly doubled the electrosorption capacitance. The MXene film itself achieved a maximum PFOA capacity of 358.5 mg g^{-1} under +1.0 V, while the MXene–

polyaniline composite reached a capacity of 966.1 mg g^{-1}. Importantly, the higher PFOA uptake reported by Zhao *et al.* relative to the O-terminated MXene of Ma *et al.* arises from differences in the film morphology and electroactive surface accessibility, rather than contradictory performance. Ma *et al.* employed densely stacked O-terminated sheets with restricted interlayer diffusion, whereas Zhao *et al.* engineered a free-standing, highly porous MXene film with enlarged gallery spacing and mixed terminations. Under an applied potential, this architecture generated stronger electric double-layer fields and exposed a significantly larger number of electroactive sites, enabling a ~66% higher adsorption capacity despite similar intrinsic $Ti_3C_2T_x$ chemistry. Another method employed by Ye *et al.*[129] involved using reductive processes with highly reactive reducing species to break down C–F bonds in PFOS. Reactive reducing species were effectively generated by the activity of heterogeneous catalysts, such as oxidized vanadium carbide (V_2C) MXene nanosheets. The process was also supported through the presence of hydrogen peroxide (H_2O_2). A degradation efficiency of 96% was achieved for PFOS (initial concentration: 50 μg L^{-1}) after 4 hours in the presence of 0.15 mg mL^{-1} V_2C MXene and 14.7 mM H_2O_2. It was better than for the process prepared with only V_2C (62% removal) or H_2O_2 alone (no removal). Near complete defluorination of PFOS (105% ± 23%) was observed after 4 hours within the V_2C and H_2O_2 process. This was followed by the formation and subsequent decomposition of a short-chain degradation product such as trifluoroacetic acid. The solvated electrons contributed to the fast defluorination of PFOS, which was adsorbed onto the V_2C MXene surface. Yang *et al.*[130] prepared mixed-dimensional MXene composite membranes, which were characterized by excellent permeability and selectivity. The membranes owed their excellent properties to the intercalation of 1D carboxylated cellulose nanofibers (CNFs) into 2D lamellar MXene nanosheets, and exhibited distinct rejection rates of over 95% for PFAS. Moreover, scientists noticed nearly an eightfold increase in permeance compared to a commercial polyamide membrane. These excellent results were achieved because of the strong hydrogen bonding interactions created during the intercalating process, which oriented the nanochannels into stable lamellar structures. These structures play a crucial role in the highly efficient permeance and molecular separation. Finally, Dixit *et al.*[123] compared the efficiency of MXenes in the removal of zwitterionic PFAS with that of anionic, nonionic, and PFAS-specific resins. The scheme of the process is presented in Fig. 10b. The obtained results showed that Ti_3C_2 MXenes were the most effective adsorbent. They achieved over 80% efficiency for all zwitterionic PFAS species within similar experimental parameters. This was compared to the tested ion exchange resins, as presented in Fig. 10c. Additionally, MXenes were the most effective medium for capturing dangerous solutions. Simultaneously, Ti_3C_2 MXene demonstrated high regeneration efficacy, which varied depending on the regenerating agent used, as shown in Fig. 1d. Scientists noted that Na_2SO_3 was the leading agent for regeneration, achieving approximately 90% recovery of zwitterionic PFAS, as shown in Fig. 10d. The scientists also investigated the formation of byproducts in a subsequent UV-sulfite experiment. The total amount of zwitterionic PFAS was decreased by approximately 65% after 6 hours (~30 J cm^{-2}), by 95% after 12 hours (~60 J cm^{-2}), and by more than 99.9% after 36 hours (~180 J cm^{-2}, see Fig. 12e). Furthermore, scientists did not observe any perfluoroalkyl carboxylates. However, they identified nine post-products of the process. All of them were formed from the UV-sulfite process of the main zwitterionic PFAS (Fig. 12f). MXenes are highly effective for the removal and degradation of PFAS due to their large surface area, tunable interlayer spacing, high conductivity, and functionalizable surfaces. They have been successfully applied in MXene-enhanced membranes, electrosorption systems, polyaniline/MXene composites, and reductive catalytic processes, achieving high removal efficiencies (>95%) and fast kinetics. Functionalization and hybridization improve the selectivity, adsorption capacity, and reusability, making MXenes a versatile and promising platform for mitigating emerging PFAS contamination in water systems.

3.4 Removal of micro- and nano-plastics (emerging contaminant)

Micro- and nanoplastics (NP) are the most prevalent global pollutants due to the excellent ductility and portability of plastic products. Human activities have generated 8.3 billion tons of plastic waste, accounting for 80% of all plastic waste. If plastic waste is not thrown away correctly, it turns into microplastics over time due to environmental conditions and microorganisms. By 2050, humanity will generate about 12 billion tons of plastic waste that will not be recycled and will pose a threat to ecosystems.[131]

Nanoplastics are a newly recognized contaminant that is widely studied in recent research. Due to their small particle size, they can penetrate cell membranes and accumulate within tissues and organs. Moreover, nanoparticles can cross biological barriers, ultimately impacting the behavior and metabolism of organisms. Additionally, the materials are excellent adsorbers for organic pollutants and heavy metal ions in aquatic environments. The materials are then transferred to other ecosystems through the food chain, impacting organisms at higher trophic levels and potentially affecting human health. However, research shows that more than 95% of microplastics can be removed from water in wastewater treatment plants. However, this is a costly and demanding process that requires the use of appropriate materials. One such material is MXene, which is used as an additive in electro-membranes to enhance the efficiency of the removal process. An innovative solution for removing nanoplastics from water was tested by Ouda *et al.*[132] The scientists employed electro-membrane filtration to remove polystyrene (PS) and polymethyl methacrylate (PMMA) at different pH levels from 5 to 9. The application of voltage resulted in an increase in the degradation to 36.9% and 29.5% for PS and PMMA, respectively. Additionally, rejection rates of up to 95.4% for PS and 97% for PMMA were achieved. The degradation efficiency of PFAS was found to be strongly dependent on pH, with varying responses observed among different PFAS species. The alkaline conditions enhance the

removal of PS, while acidic conditions are more favorable for PMMA. Yang *et al.*[131] also utilized a membrane system to remove PFAS from wastewater systems. For this purpose, scientists etched Co_3O_4 nanoparticles embedded within holey $Ti_3C_2T_x$ MXene (Fig. 11a–d). Finally, simple vacuum filtration was used for polymeric membranes as a supporting matrix for the fast degradation of microplastics from pollutants. The prepared system was tested by utilizing fluorescent polystyrene microspheres of various sizes. The membranes showed exceptionally high microplastic removal rates, reaching more than 99.3%. Adding MXenes to the membranes allowed for greater water flow. This also helped maintain the high microplastic removal efficiency due to the physicochemical stability of the membranes. A novel approach to removing nanoplastics was introduced by Urso *et al.*,[133] who designed multifunctional MXene-derived oxide microrobots. These microrobots can capture nanoplastics "on-the-fly" in three-dimensional (3D) space by quickly drawing them to their surfaces. This unique capability allows them to form multilayer stacks for easy magnetic collection. The process begins with the thermal annealing of $Ti_3C_2T_x$ MXene to convert it into photocatalytic multilayered TiO_2. Then, a platinum (Pt) layer is added, along with magnetic γ-Fe_2O_3 nanoparticles. Finally, MXene-derived γ-Fe_2O_3/Pt/TiO_2 microrobots can move efficiently without fuel when it is exposed to light irradiation due to their negative photogravitaxis. Another method to remove microplastics from wastewater is photocatalysis. This method is highly efficient with environmentally friendly properties, such as the production of hydrogen (H_2). Cao *et al.*[134] prepared MXene/$Zn_xCd_{1-x}S$ composites with integrated photocatalytic properties for H_2 evolution and the simultaneous removal of polyethylene terephthalate (Fig. 11e). The obtained composites showed brilliant photocatalytic performance and H_2 evolution rate (14.17 mmol g^{-1} in alkaline PET solution). Furthermore, polyethylene terephthalate was converted into useful organic micromolecules, especially glycolate, ethanol, *etc.* The high efficiency of the materials is caused by their improved ability to separate photocarriers and their optimized band structure. To achieve higher efficiency in PFAS decomposition, MXenes were added to various materials to obtain novel composites. Yang *et al.*[135] used a hydrothermal method to prepare Ti-based MOF catalysts with abundant Ti–O_x bonds and graphitic carbon with a porous structure. The O–Ti–O species and graphitic carbon facilitated the application of materials in photosensitive and catalytic processes. Scientists used composites in the sonication process and noted that ultrasound effectively removed microplastics. The obtained results show over 75% removal of micro-polyethylene after 4 hours of the sonocatalytic process. MXenes and MXene-based composites are highly effective in removing micro- and nano-plastics due to their large surface area, tunable interlayer spacing, and excellent physicochemical stability. They have been successfully applied in electromembrane systems, photocatalytic composites, and MXene-derived microrobots, achieving high removal efficiencies (>95%) and enabling simultaneous degradation or transformation of plastics into useful byproducts. Functionalization, hybridization, and integration with magnetic or catalytic components further enhance the removal efficiency, scalability, and reusability, making MXenes a promising solution for emerging plastic pollutants in water systems.

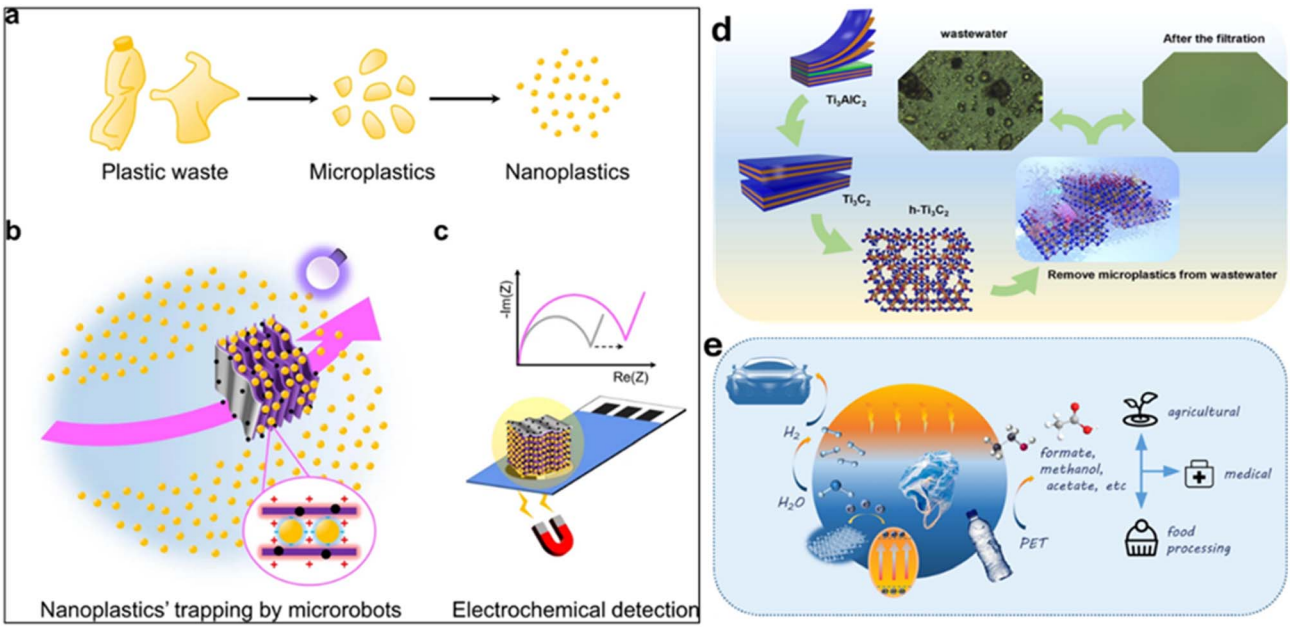

Fig. 11 Scheme of the (a) formation of micro- and nano-plastics from plastic waste fragments in water. (b) Microrobots removing nanoplastics from water by trapping them onto their surfaces. (c) Nanoplastic detection by microrobots using electrochemical impedance spectroscopy. (d) Microplastic removal using membranes containing MXene flakes. Reprinted from ref. 131 with permission from Elsevier, *J. Colloid Interface Sci.*, Copyright 2022. (e) Removal of micro- and nano-plastics *via* the photocatalysis process. Reprinted from ref. 132 with permission from Elsevier, *Chem. Eng. J.*, Copyright 2024.

3.5 Pharmaceuticals removal

MXenes have a high surface area, electrical conductivity, and adjustable surface functionalities, and they can absorb and break down pharmaceutical waste.[136,137] The primary purpose of the $Ti_3C_2T_x$ nanosheet-based hybrid photocatalyst was to eliminate carbamazepine, an antiepileptic medication that typically finds its way into water bodies and harms aquatic ecosystems.[138] By creating a heterostructure with Schottky connections that permitted controlled oxidation under UV light, carbamazepine was successfully broken down. It worked very well for the process at low pH levels (between 3 and 5). Other environmental factors, in addition to material ones, may improve MXene's degradation function.[138] In another study, Ti_3C_2 has been shown to break down the antiepileptic medication carbamazepine effectively in the presence of visible light, indicating that it may be useful in treating drug-contaminated water.[139] An additional typical medicine that is detected in water supplies is the anti-inflammatory medication diclofenac. Using a single-step chemical co-precipitation method, magnetic $Ti_3C_2T_x$ was synthesized for the photocatalytic degradation of diclofenac in a UV/chlorine system. The outstanding first-order rate constant for the UV/chlorine process, which is superior to those of the traditional UV and UV/H_2O_2 techniques, is the result of the created active radicals.[138] To further improve their photocatalytic degradation effectiveness, MXenes have been coupled synergistically with a variety of materials, such as graphene, MOFs, polymers including cellulose and chitosan, and carbon nanotubes.[140] By utilizing the complementary qualities of the added materials with the special qualities of MXenes, these composite systems open new possibilities for environmental remediation and photocatalysis technologies. Creating an oxidation method employing MXene nanosheets to produce intercalated TiO_2 in graphene oxide-based nanofiltration membranes is one of the most remarkable examples. The composite of Ti_3C_2 with graphitic carbon nitride (g-C_3N_4) and TiO_2 is another notable example of MXene synergy.[140] These constituents demonstrated mutually reinforcing effects and robust interactions, culminating in the amplified absorption of visible light and expedited separation of photo-generated carriers, hence augmenting the rate of photocatalytic destruction. The high photocatalytic degradation efficiency in MXene-based photocatalysts can only be achieved by improved charge separation and reduced recombination, which makes them a viable option for purifying water. MXene/ZnO composites were found to have considerably increased photocatalytic activity under visible light compared to ZnO alone in another work.[141] This was due to enhanced light absorption and charge separation capability. MXenes and MXene-based composites are highly effective in the removal and degradation of pharmaceutical contaminants due to their large surface area, tunable surface chemistry, and excellent charge transport properties. They have been applied in photocatalytic degradation systems for drugs like carbamazepine and diclofenac, achieving high degradation efficiencies under UV or visible light. Synergistic integration with materials such as graphene, MOFs, TiO_2, g-C_3N_4, and ZnO enhances the light absorption, charge separation, and overall photocatalytic performance, making MXene-based systems promising for sustainable pharmaceutical wastewater remediation.

4 Mechanisms involved in the removal of heavy metals, dyes, and radionuclides

Different mechanisms describe the adsorption phenomena of heavy metals on the surface of MXenes. Due to the large surface area of the MXene layers, the metal ions may be trapped within them. Additionally, ion exchange occurs between the metal ions and the groups present on the MXene surface, which leads to electrostatic interactions between them. The titanium present in the MXene itself has excellent affinity toward many ions. In most cases, the Freundlich model is used to describe multilayer adsorption for the removal of metal ions.

The adsorption mechanism of Cr(VI) ions by MXene ($Ti_3C_2T_x$) nanosheets using the reduction adsorption method is shown in Fig. 12c. The presence of hydroxyl ions at low pH values is high because the MXenes are positively charged and attract $Cr_2O_7^{2-}$ (negatively charged) *via* electrostatic interaction.[44] There is a reduction in Cr, which changes Cr(VI) to Cr(III) after the sorption process. The process involves the transfer of an electron from the surface of the MXene nanosheets to Cr(VI). Finally, the reduced Cr(III) ions adsorb on the surface with a high adsorption rate towards metallic ions, which is plausibly due to the production of the Ti–O bond. Covalent bonding occurs, which forms a Ti–O–Cr(III) bond.

The removal of dyes on the surface of the MXenes arises mainly because of the interaction of various functionalities present on the MXene surface and the dye molecules. The –OH groups present on the Ti surface are possibly attached to the MB^+ molecules. Because of this, a monodentate complex forms *via* M–O–H–N bond,[142] as shown in Fig. 12b, and the equations for the interaction of MB and hydroxyl are shown below.

$$TiOH \leftrightarrows Ti^{-}O^{-} + H^{+}$$

$$Ti^{-}O^{-} + MB^{+} \leftrightarrows TiO - MB$$

The removal of MB using $Ti_3C_2T_x$ happens *via* adsorption and succeeding photocatalytic decomposition, which includes various steps. In step one, the $Ti_3C_2T_x$ surface adsorbs MB molecules, which probably increases the stacking disorder, possibly because of chemical MXene transformation or compression of the layered structure, followed by the formation of titania due to oxidation of MXene. The $Ti_3C_2T_x$ sheets can facilitate the reduction of MB molecules, and adsorption onto the MXene@Fe_3O_4 eventually occurs due to the OH and Ti interactions. The production of the OH–N bond appears due to the dipole–dipole hydrogen bonding interaction between Ti–OH and N of the MB molecule. There are three stages that occur due to the adsorption. The first step involves the sorption of the particle onto the adsorbent's external surface. The second step

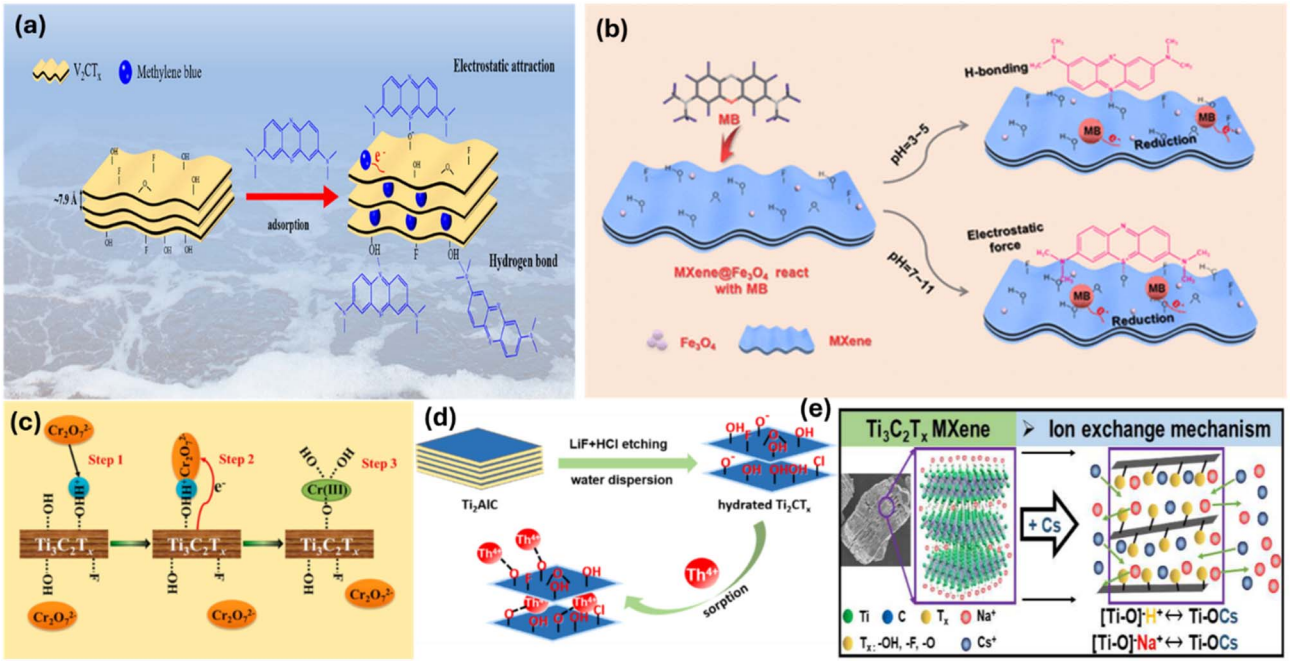

Fig. 12 (a) Removal mechanism of MB using V_2CT_x. Reprinted from ref. 144 with permission from the American Chemical Society, the *J. Phys. Chem. Lett.*, Copyright 2020. (b) Representation of the removal mechanism of MB using MXene@Fe_3O_4. Reprinted from ref. 142 with permission from the American Chemical Society, *Appl. Mater. Interfaces*, Copyright 2019. (c) Adsorption mechanism of Cr(VI) by $Ti_3C_2T_x$. Reprinted from ref. 44 with permission from the American Chemical Society, *Appl. Mater. Interfaces*, Copyright 2015. (d) Thorium adsorption mechanism onto the $Ti_3C_2T_x$ surface. Reprinted from ref. 18 with permission from Elsevier, *Chem. Eng. J.*, Copyright 2019. (e) Proposed mechanism of Cs^+ remediation by MXene sheets. Reprinted from ref. 101 with permission from Elsevier, *J. Nucl. Mater.*, Copyright 2020.

involves the internal diffusion of the particles, followed by obtaining the adsorption equilibrium. In a recent study, V_2CT_x MXene has been shown to efficiently adsorb organic dye pollutants through a combination of strong coulombic interactions, hydrogen bonding, and π–π stacking with the aromatic moieties of the dyes. Molecular dynamics simulations reveal that adsorption is spontaneous and selective, with interaction energies of up to −150 kJ mol^{-1}, highlighting the high affinity of cationic dyes. Factors such as the molecular charge, linearity, and mass further modulate the adsorption efficiency, establishing MXenes as versatile and robust substrates for aqueous pollutant removal.[143]

Another mechanism[144] shows the coulombic interaction between MB^+ and negatively charged V_2CT_x (see Fig. 12a). The reaction takes place in slightly acidic media, as shown below.

$$–VOH \leftrightarrow –VO^- + H^+$$

$$–VO^- + MB \leftrightarrow –VO^- MB^+$$

The remediation of the radionuclides happens because of electrostatic attraction and ion exchange between the radionuclides and the MXene surface. The mechanism of Th(IV) adsorption on the hydrated $Ti_3C_2T_x$ is demonstrated in Fig. 12d. The intense attraction between Th(IV) and Ti–OH was confirmed by XPS analysis.[18] Proton exchange due to the elevation in the amount of H^+ ions shows the formation of the Ti–O–Th bond through the adsorption process. Generally, the chemical ion exchange predominates when the free energy ranges between 8–16 kJ mol^{-1}. The free energy for Ba^{2+} and Sr^{2+} was 808 and 11 kJ mol^{-1}, confirming the establishment of the ion-exchange mechanism. The ion exchange process was responsible for the adsorption of Cs^+ onto the MXene surface (see Fig. 12e). The other background ions also take part in the remediation process. The sorption capacity was 148 mg g^{-1}, and the adsorption phenomena support the ion-exchange mechanism.[101] Additionally, in another study, a $Ti_3C_2T_x$–Fe_3O_4 (70 : 30) composite was found to efficiently remove radionuclides ^{133}Ba and ^{137}Cs through a combination of encapsulation and surface complexation. Optimized adsorption occurred at pH 5.5–8.0, with maximum capacities of 6.34 mmol g^{-1} for Cs^+ and 4.18 mmol g^{-1} for Ba^{2+}.[145] The high affinity for Cs^+ is attributed to increased interlayer spacing within MXene, while the synergistic effect of Fe_3O_4 enhances the structural stability and adsorption performance. This work demonstrates the potential of MXene-based composites for the selective removal of hazardous ions from aqueous environments. MXenes remove heavy metals, dyes, radionuclides, PFAS, micro/nanoplastics, and pharmaceuticals through a combination of mechanisms, including adsorption, ion exchange, electrostatic interactions, surface complexation, reduction, and photocatalytic degradation. Their high surface area, layered structure, and tunable surface functional groups (–OH, –O, –F) enable strong binding and selective uptake of contaminants. For dyes and organics, MXenes also facilitate photocatalytic or advanced oxidation

processes. Meanwhile, for PFAS and plastics, they enhance electrosorption and membrane-based removal. Overall, the versatility and physicochemical properties of MXenes make them highly effective for environmental remediation across a wide range of pollutants.

5 Renewal/reuse capability of MXene- and MXene-based materials

A variety of reports show that MXenes and MXene-related materials retain excellent stability, and can be used for several cycles after the adsorption of the pollutants (dye, heavy metal, or radionuclides) from the water. The magnetic MXenes (due to the incorporation of iron nanoparticles) have shown excellent recyclability after the adsorption process of mercury ions from the water.[91] The efficiency of removing the Hg(II) ions was retained at more than 90% for up to four consecutive cycles. Another study showed that the encapsulation of iron on MXenes will enhance their stability, and a magnet can collect these composite materials after the adsorption process. The collected MXene@Fe_3O_4 composite was dried and reused,[146] which demonstrated a removal efficiency of 77% after five consecutive cycles. The MXenes ($Ti_3C_2T_x$) loaded with Cs^+ were regenerated (*via* 0.2 M HCl solution) and reused for up to 5 consecutive cycles with minimal decline of the removal efficiency.[100]

The removal of contaminants (dyes, heavy metals, and medications) from MXene-related sorbents and the possibility of their subsequent reutilization are critical measures in cost control, risk reduction for the environment, and handling the problem of disposing toxic sludge. Information on the desorption of adsorbed pollutants from MXene-derived adsorbents using a range of eluents, including HCl, HNO_3, NH_4OH, H_2SO_4, Na_2CO_3, NaOH, KOH, and DI-water, is available in the literature.[147,148] Through a simple batch reaction approach, Ghani *et al.*[147] created a sodium-intercalated $Ti_3C_2T_x$ (SI $Ti_3C_2T_x$) MXene, which functions as a sorbent and can then be used in remediation and electrochemical regeneration outcomes. The findings suggest that an intercalation method occurred, causing the "*d*" spacing of the MXene to expand. This resulted in a much higher adsorption capacity than that of virgin $Ti_3C_2T_x$ MXene and most comparable nanostructures that have been documented in previous research. The improved adsorption capacity of SI–$Ti_3C_2T_x$ is supported by this increase in spacing. Moreover, it was discovered that the intercalation procedure made it easier to substitute single-bond oxygen and single-bond hydroxyl groups for single-bond fluoride terminations. SI–$Ti_3C_2T_x$ MXene showed exceptionally quick kinetic rates that were consistent with the Elovich kinetic model. The Redlich–Peterson isotherm model was followed by the adsorption isotherm, suggesting a possible chemisorption mechanism. This mechanism, which is controlled by rate-controlling stages, may be explained by the electrostatic attraction between the adsorbent and adsorbate. Complete elimination of the adsorbate (ciprofloxacin: CPX) was made possible by the fast electrochemical regeneration rates of SI–$Ti_3C_2T_x$, which are attributed to its high electrical conductivity. These studies suggest that MXene-related adsorbents have great potential for effective use. They possess the capability for recycling and the recovery of metal ions, in addition to exhibiting extraordinary potential for the elimination of heavy metals. Table 1 provides information on different MXene-based materials for the remediation of different pollutants. Additionally, Table 2 provides a comparative overview of MXenes and other leading material classes used in water remediation, highlighting key differences in their performance, scalability, and environmental impact. The analysis clearly shows that while several materials exhibit strong remediation capabilities, MXenes offer a unique balance of high efficiency, tunable chemistry, and emerging scalable green synthesis routes, positioning them as a compelling next-generation platform. Overall, MXenes' stability, rapid kinetics, and regeneration potential make them cost-effective, environmentally friendly, and practical for repeated use in pollutant removal.

6 Challenges and other applications

Even though these MXenes exhibit extraordinary performance in the adsorption of pollutants from water, there remain numerous challenges that still need to be addressed to achieve the full exploitation of their properties. One of the significant challenges is the high cost and low yield in production. Presently, MXenes are produced with a small yield at a lab scale. A system should be designed to achieve a significantly large-scale output that is both efficient and environmentally friendly. This will be further helpful in the advanced research field and introduce viable applications of MXenes on an industrial scale. It is considered that large-scale production will reduce costs. The traditional method uses HF to prepare MXenes, which is hazardous and is connected with severe health and environmental problems. The substitution of HF with less toxic or green chemicals may provide an eco-friendly approach for MXene production. To date, a top-down approach has been the primary method through which the MXenes are predominantly synthesized. There are few reports on the output of MXene utilizing a bottom-up approach. Further research is necessary in this direction to survey the unfamiliar bottom-up techniques for the fabrication of MXenes. Another barrier for researchers to overcome is the storage of MXenes, which require sub-zero temperatures. So, there is a need to develop an effective process for preserving MXene solutions over a longer time period without being oxidized. The use of MXenes in different applications necessitates further exploring their toxic effects on human health, the environment, and other living organisms. Aggregation is also a problem that can reduce the impact of adsorption and the surface area of MXenes. Surface modification and the chemistry behind the process of removing pollutants from the water must be thoroughly explored. Surface enhancement increases stability, and biocompatibility reduces cytotoxicity and increases recyclability for MXenes. Even though $Ti_3C_2T_x$ is frequently used in water-related applications, it is necessary to develop new MXenes and explore different adsorption applications. MXenes and related composite materials have been satisfactorily used in applications, including as

Table 1 Summary of the application of MXenes in the remediation of different contaminants

Type of MXenes	Contaminant	Adsorption capacity	References
MXene/alginic acid composite	Cu(II)	87.6 mg g^{-1}	149
MXene/alginic acid composite	Pb(II)	382.7 mg g^{-1}	149
$Ti_3C_2T_x$-KH570	Pb(II)	147.29 mg g^{-1}	150
MXene (Ti_3C_2)/PEI functionalized sodium alginate aerogel	Cr(VI)	538.97 mg g^{-1}	151
MXene–CS composites	Cr(VI)	43.1 mg g^{-1}	152
Oxygenated MXene	Hg(II)	1057.3 mg g^{-1}	153
MoS_2/MX-II	Hg(II)	1435.20 mg g^{-1}	154
MXene-45	Pd(II)	184.56 mg g^{-1}	155
Alk-Ti_2C sheet	Cd(II)	325.89 mg g^{-1}	156
Alk-MXene/LDH	Ni(II)	222.7 mg g^{-1}	157
$Ti_3C_2T_x$	As(III)	2.8 mg g^{-1}	158
Sodium alginate/MXene/$CoFe_2O_4$ under RMF	Ciprofloxacin	290.91 mg g^{-1}	159
SI (sodium ions)–$Ti_3C_2T_x$	Metformin	145.07 mg g^{-1}	159
Cobalt-doped $ZnTiO_3$/$Ti_3C_2T_x$	Tetracycline	14.9 mg g^{-1}	160
Sonicated $Ti_3C_2T_x$ MXene	Amitriptyline	58.7 mg g^{-1}	161
DSP-M ($Ti_3C_2T_x$ and DASNP)	Naproxen	166.71 mg g^{-1}	162
Ti_3C_2@Fe_3O_4@β-CD	Doxorubicin	7.35 μg mg^{-1}	163
MXene-PEDOT:PSS	Perfluorohexanoic acid (PFHxA)	45.6 mg g^{-1}	164
MXene-PEDOT:PSS	Perfluorooctanoic acid (PFOA)	51.1 mg g^{-1}	164
MXene-PEDOT:PSS	Perfluorononanoic acid (PFNA)	54.9 mg g^{-1}	164
O-terminated MXene	Perfluorooctanoic acid (PFOA)	215.9 mg g^{-1}	165
Cl–MXene	Perfluorooctanoic acid (PFOA)	117.3 mg g^{-1}	165
F-terminated MXene	Perfluorooctanoic acid (PFOA)	158.8 mg g^{-1}	165

an antibacterial agent and for capacitive deionization. The study report shows that MXenes exhibit antifouling and antibacterial characteristics when modified with silver nanoparticles. MXenes are also used in CDI because of their high hydrophilicity and electrical conductivity.[171] The tunable surface area is also an essential parameter to the usage of MXenes in CDI. These MXene-based electrodes in CDI applications have shown extraordinary adsorption capacity for the simultaneous adsorption of cations and anions. Studies have also demonstrated the unique antibacterial properties of MXenes against bacteria.[172] The anionic nature of the surface of the MXenes is responsible for the direct killing of the bacteria

Table 2 Comparison of MXenes and leading material platforms for water remediation

Material	Performance in water remediation	Scalability	Environmental impact	Ref.
MXenes	Very high: metallic conductivity, hydrophilicity, abundant surface groups (–O, –OH, –F) enable adsorption, redox activity, and catalysis	Good potential: top-down etching from MAX phases; scalable with reactor volume. Emerging greener synthesis methods (molten-salt, electrochemical)	Moderate to high concern: HF or fluoride etchants traditionally used, but green routes are being developed. Long-term stability improved	166
Graphene (and derivatives)	Good conductivity and surface area; lacks rich surface chemistry, limiting intrinsic redox/adsorption	Scalable *via* liquid-phase exfoliation; CVD possible but costly	Production can involve strong acids, hazardous solvents, nanoparticle release risk, and energy-intensive processes	167
MoS_2/TMDs	Good for membranes, catalysis, and adsorption. Membranes show high ion rejection and flux; catalytically active when combined (*e.g.*, MoS_2/Ti_3C_2 for HER)	Exfoliation and CVD routes exist, but scaling with defect control is nontrivial. Large-area membranes are challenging	Generally benign, but the synthesis method determines footprint; stability in aqueous media varies; some require high temperature or vacuum growth	168
MOFs (2D & 3D)	Extremely high surface area, tunable porosity, good for adsorption/catalysis of metals and organics	Scalability challenging: solvothermal synthesis hard to scale. Green methods emerging (mechanochemical, electrochemical)	Significant concerns: organic solvents (DMF) toxic, energy-intensive; water stability variable, lifecycle assessments limited	169 and 170

because of the hydrogen bonding between the oxygenated groups of MXenes and the cell membrane, which then prohibits nutrient intake. The atomic configuration and structure also play a critical part in the antibacterial characteristics of MXenes. The surface tuning of MXenes can also be beneficial for sensing-based applications. Data based on the DFT calculations reveal that the Ti_2CT_x monolayer containing oxygen groups was sensitive towards ammonia (NH_3) and correspondingly to other gases.[173] Additionally, the doping of metal nanoparticles into MXenes will increase the sensing ability of the MXenes by enhancing the catalytic activity. MXenes have also been used as the sensor for phenols by the electrochemical process. Another application of MXenes is electromagnetic interference (EMI) shielding.[174] Studies demonstrated that MXenes were explored for EMI because of their superior interlayer electronic coupling and excellent electrical conductivity. The interlayer structure of MXenes allows the radiation to go for multiple internal reflections, followed by the absorption of electromagnetic waves.

Despite their exceptional adsorption capabilities for hazardous pollutant removal, MXenes face critical barriers that hinder large-scale application. These challenges include limited compositional tunability, high synthesis costs, and the lack of scalable production methods. Currently, MXenes are largely confined to laboratory-scale preparation with modest yields. Advancing economically viable and environmentally sustainable manufacturing technologies will be essential to unlock their industrial and commercial potential. For large-scale production, a relatively low price is anticipated. It is essential to investigate MXene's potential as an adsorbent in continuous operation systems. Moreover, several theoretical studies, like DFT, have forecasted the remarkable properties of MXenes in water treatment procedures. Appropriate research and the growth of a functional system are needed to validate the outcomes of these theoretical computations. Seldom have MXene membranes been studied for environmental pollutant removal. Most MXene membranes have demonstrated exceptional quality and selectivity when utilized to stop different types of water pollutants from penetrating. The main issues include grain boundaries, impurities, defects, or residues of molecules that clog the pores of the nanolayers and lower the gas flow rate. For this reason, the mixture needs to be carefully filtered before passing through the membrane system. Furthermore, it is uncertain how dangerous combinations and pollutants are chosen for remediation. Thus, before anticipating the mechanism of selectivity, a thorough understanding of the elements influencing the separation process is necessary. Research on the possible applications of MXenes in capacitive deionization, antimicrobials, adsorbents, and membranes—aside from adsorption—is scarce. Further research in this area is necessary to determine novel applications of these fascinating 2D nanomaterials in water filtering. There is a good chance that items based on MXene will soon be available for purchase.

Reproducibility of MXene synthesis and performance remains a major challenge because small variations in the MAX-phase precursor purity, etching conditions, and post-treatment steps can drastically alter the surface terminations, defect densities, interlayer spacing, and flake morphology. For example, standard wet-chemical fluoride-based etching often yields heterogeneous mixtures of –F, –OH, and –O terminations, while alternative routes, such as molten-salt electrochemical etching, enable the deliberate production of fluorine-free, –Cl/–O/–S terminated MXenes, offering greater consistency. Low-temperature molten-salt (LTMS) etching has recently demonstrated that high-quality MXenes (*e.g.*, $Ti_3C_2T_x$) can be prepared in as little as 5 minutes and scaled up to >100 g per run, facilitating rapid, large-scale production while maintaining reproducible structural and electrochemical properties.[175,176] Nevertheless, reproducibility still suffers from batch-to-batch variability arising from differences in MAX precursor quality (stoichiometry, grain size), subtle changes in intercalation/delamination procedures, washing pH and volumes, and lack of standardization in reporting these parameters. Enhancing reproducibility, therefore, requires the adoption of automated or continuous-flow synthesis platforms with real-time monitoring (*e.g.*, pH, intercalant concentration, interlayer spacing), development of community-wide standards for precursor quality and reporting (composition, etchant, time, temperature, and washing), and generation of open datasets linking synthesis parameters → surface chemistry → material performance.[177] Furthermore, controlled termination engineering *via* post-etching treatments (*e.g.*, plasma and salt-based functionalization) or alternative "bottom-up" routes, such as direct chemical vapor deposition or gas-phase etching, together with rigorous *in situ* diagnostics, appears essential for producing MXenes with reproducible, application-ready properties at scale. Finally, implementing solvent/salt recycling and less-toxic chemistries will not only make synthesis safer and greener, but also reduce batch-to-batch variability due to reagent purity or waste-induced contamination. Based on the most recent promising results, it is sensible to believe that MXenes may be the next-generation materials for environmental cleanup and water desalination. It will be necessary to overcome the current difficulties and develop better MXene-based membranes by refining their synthesis methods, as the morphology and structure of the MXene membranes affect their performance. Additionally, the rapid production (within minutes) of MXene-based membranes with the use of a unique electrophoretic deposition (EPD) technique, which involved depositing negatively charged MXenes on an anode to generate 2D membranes. This membrane synthesis method is easier, faster, and uses less power than other procedures. These advantages make this approach viable for the production of MXene-based membranes for ion separation and removal. Thus, scientists may possibly further reduce the difficulties by creating more effective synthesizing strategies and processes. By adding polymers to its surface, the stability and separation capabilities of MXenes can be enhanced in yet another way. In comparison to MXene/traditional 2D materials, MXene/polymer membranes function exceptionally well. Naturally, the prohibitively high cost of MXenes in membranes will determine its commercialization and limitations. Currently, the need to use the lowest amount of material may be satisfied *via* ultrathin and mixed matrix membranes. For instance, because GO and MXenes have

different interlayer spacings, combining GO and MXenes would produce an organized layer-structured membrane, which can balance the molecular repulsion of organic pollutants and the permeability of water and organic solvents.[178,179] Despite the outstanding performance of MXenes in pollutant adsorption, several challenges must be addressed to fully realize their potential. Persistent challenges include costly and low-yield synthesis, dependence on hazardous chemicals such as HF, instability during storage, and aggregation-induced performance deterioration. Overcoming these barriers will necessitate the implementation of sustainable large-scale manufacturing routes and improved stabilization protocols. Surface modification can enhance stability, recyclability, biocompatibility, and adsorption efficiency, while novel MXenes beyond $Ti_3C_2T_x$ should be explored. Beyond adsorption, MXenes show strong potential in antibacterial applications, capacitive deionization, sensing, and EMI shielding due to their tunable surface chemistry and high conductivity. Advances in membrane fabrication, including electrophoretic deposition and MXene-based composites, are enabling more efficient water purification technologies. Overall, MXenes are a promising platform for next-generation environmental remediation and water treatment. However, the cost, scalability, and material optimization remain critical for commercialization.

7 Critical assessment & risk mitigation of MXenes in environmental use

Despite the promising performance of MXenes (especially $Ti_3C_2T_x$) in water remediation, there are legitimate environmental and health concerns that deserve rigorous scrutiny. Recent studies show that $Ti_3C_2T_x$ can exert ecotoxicity toward aquatic organisms even at sublethal concentrations: for instance, exposure of *Daphnia magna* to $Ti_3C_2T_x$ caused extensive metabolomic perturbations (hundreds of metabolites altered), implicating lipid, amino acid, and energy-metabolism pathways despite no overt mortality or growth inhibition. Similarly, toxicity tests on *Microcystis aeruginosa* revealed that $Ti_3C_2T_x$ significantly impaired growth and photosynthetic capacity at higher concentrations ($\geq$5 mg L^{-1}), indicating oxidative stress and metabolic disruption.

A major environmental risk arises from the instability of MXenes in aqueous or oxidative atmospheres: upon exposure to water/air, $Ti_3C_2T_x$ can degrade into titanium dioxide (TiO_2) nanoparticles and carbonaceous fragments. Such degradation products may themselves have unknown or harmful ecotoxicological properties, for example, ROS generation, bioaccumulation, or altering sediment chemistry. In addition, studies suggest that chronic exposure (*e.g.*, *via* repeated release or sludge disposal) of MXene or its byproducts could pose cumulative ecological or health risks. On the human health side, *in vivo* experiments have shown that Ti_3C_2 nanosheets can disrupt spermatogenesis in male mice *via* induction of oxidative stress, DNA damage, and activation of apoptosis through the ATM/p53 pathway.[178] Despite their promising performance in water remediation, the large-scale deployment of MXenes warrants caution due to potential environmental risks. Strategies to mitigate adverse effects include surface functionalization or immobilization of MXenes within stable matrices, such as polymers, membranes, or composites, to limit leaching and the release of free flakes. Controlled dosing at concentrations below ecotoxic thresholds can further minimize biological impacts. Meanwhile, thorough life cycle and environmental fate assessments encompassing the degradation pathways, byproducts (like TiO_2) and long-term bioaccumulation are essential. Post-treatment stabilization or the capture of MXene residues ensures that treated water and waste sludges do not contribute to environmental contamination. Additionally, engineering oxidation-resistant or biodegradable MXenes through tailored surface terminations, passivation layers, or composite stabilization can enhance their durability, while reducing ecological risks. Overall, while MXenes offer exciting capabilities for water remediation, their environmental and health safety profile remains incomplete. For responsible deployment, combining rigorous ecotoxicological testing, careful materials engineering, and containment strategies is essential; failure to do so risks substituting one pollution problem (organic/metal contaminants) with another (nanomaterial pollution).

8 Future directions

Emerging research on MXenes for water remediation emphasizes the importance of green and solvent-free synthesis strategies. Traditional HF-based etching methods, while effective, pose significant environmental and safety concerns, limiting the large-scale application of MXenes. Alternative approaches such as molten-salt etching, electrochemical etching, and mechanochemical synthesis have shown promise in producing MXenes with tunable surface terminations (*e.g.*, –Cl, –O, and –S) in a more environmentally friendly manner. These methods not only reduce hazardous waste but also improve reproducibility and facilitate scale-up, which is crucial for practical deployment in water treatment systems. Future work should continue to optimize these green synthesis protocols, focusing on controlling the flake size, interlayer spacing, and surface chemistry to maximize performance, while minimizing the chemical footprint. Integration of MXenes into composite systems is another key direction. MXene–polymers, MXene–nanocelluloses, and MXene–carbon-based composites offer synergistic advantages, combining the high surface area, conductivity, and active sites of MXenes with the mechanical robustness and antifouling properties of the matrix. Such composites have demonstrated enhanced removal of heavy metals, pharmaceuticals, and persistent organic pollutants. For PFAS remediation, MXene-based thin-film nanocomposite membranes have achieved high rejection efficiencies (>96%), while maintaining good flux. Future research should explore functionalization and hybridization with other 2D materials (*e.g.*, MOFs and graphene) to further improve the selectivity, durability, and regeneration under realistic water conditions. Addressing microplastics, MXenes can be incorporated into 3D scaffolded membranes or cryogel-based composites that enable dynamic capture, self-cleaning, and reusability. The high hydrophilicity,

conductivity, and tunable surface chemistry of MXenes make them suitable for integrating stimuli-responsive or electrically assisted filtration systems, which can enhance microplastic capture and reduce fouling. Additionally, life-cycle assessments and techno-economic studies are critical to evaluate the sustainability and cost-effectiveness of these systems. Standardized synthesis, characterization, and testing protocols will also be necessary to ensure reproducibility, batch-to-batch consistency, and comparability across studies, which is essential for translating laboratory advances into scalable water remediation technologies.

9 Conclusion

MXenes represent a transformative class of 2D materials with exceptional structural versatility, tunable surface chemistry, and outstanding physicochemical properties, positioning them as next-generation solutions for environmental remediation. Their derivatives demonstrate remarkable efficacy in the adsorption and degradation of dyes, heavy metals, radionuclides, PFAS, and micro- and nano-plastics. Tailored functionalization and controlled oxidation further enhance selectivity and efficiency, enabling targeted interactions with diverse contaminants. $Ti_3C_2T_x$ and Ti_3CN MXenes have been extensively explored, exhibiting high adsorption capacities, recyclability, and potential biocompatibility, indicating pathways toward sustainable, cost-effective water purification. However, challenges such as oxidative instability, limited scalability, and performance variability over repeated cycles remain critical barriers to industrial implementation. Future research must address the development of a large-scale, environmentally sustainable synthesis approach, advanced surface engineering for selective contaminant capture, and integration of MXene-based systems into existing water treatment infrastructures. Rigorous assessment of the environmental and human health risks, alongside regulatory frameworks, is essential. With interdisciplinary innovation, MXenes offer a versatile, high-performance platform capable of transforming water purification and addressing pressing global pollution challenges.

Conflicts of interest

There are no conflicts to declare.

Data availability

No primary research results, software or code have been included and no new data were generated or analysed as part of this review.

References

1 D. J. MacAllister, A. M. MacDonald, S. Kebede, S. Godfrey and R. Calow, Comparative performance of rural water supplies during drought, *Nat. Commun.*, 2020, **11**, 1–3.
2 S. K. Raj, A. J. Carrier, B. C. Youden, M. R. Servos, K. D. Oakes and X. Zhang, Electrochemical techniques for uranium extraction from water, *Chem. Eng. J.*, 2024, **17**, 152341.
3 R. Ghanbari and E. N. Zare, Engineered MXene–polymer composites for water remediation: promises, challenges and future perspective, *Coord. Chem. Rev.*, 2024, **518**, 216089.
4 K. H. Aziz, Removal of toxic heavy metals from aquatic systems using low-cost and sustainable biochar: a review, *Desalin. Water Treat.*, 2024, **320**, 100757.
5 K. H. Aziz, F. S. Mustafa, M. A. Karim and S. Hama, Biochar-based catalysts: an efficient and sustainable approach for water remediation from organic pollutants *via* advanced oxidation processes, *J. Environ. Manage.*, 2025, **390**, 126245.
6 S. K. Raj, V. Sharma, A. Yadav, P. D. Indurkar and V. Kulshrestha, Nano-alumina wrapped carbon microspheres for ultrahigh elimination of pentavalent arsenic and fluoride from potable water, *J. Ind. Eng. Chem.*, 2023, **117**, 402–413.
7 M. Bagheri and S. A. Mirbagheri, Critical review of fouling mitigation strategies in membrane bioreactors treating water and wastewater, *Bioresour. Technol.*, 2018, **258**, 318–334.
8 R. Das, C. D. Vecitis, A. Schulze, B. Cao, A. F. Ismail, X. Lu, J. Chen and S. Ramakrishna, Recent advances in nanomaterials for water protection and monitoring, *Chem. Soc. Rev.*, 2017, **46**, 6946–7020.
9 M. Sun and J. Li, Graphene oxide membranes: functional structures, preparation and environmental applications, *Nano Today*, 2018, **20**, 121–137.
10 S. K. Raj, V. Yadav, G. R. Bhadu, R. Patidar, M. Kumar and V. Kulshrestha, Synthesis of highly fluorescent and water-soluble graphene quantum dots for detection of heavy metal ions in aqueous media, *Environ. Sci. Pollut. Res.*, 2020, **13**, 1–7.
11 A. Rajput, S. K. Raj, P. P. Sharma, V. Yadav, H. Sarvaia, H. Gupta and V. Kulshrestha, Synthesis and characterization of aluminium modified graphene oxide: an approach towards defluoridation of potable water, *J. Dispersion Sci. Technol.*, 2018, **8**, 1101–1109.
12 S. K. Raj, A. Rajput, H. Gupta, R. Patidar and V. Kulshrestha, Selective recognition of Fe^{3+} and Cr^{3+} in aqueous medium *via* fluorescence quenching of graphene quantum dots, *J. Dispersion Sci. Technol.*, 2019, **40**, 250–255.
13 V. Yadav, S. K. Raj, N. H. Rathod and V. Kulshrestha, Polysulfone/graphene quantum dots composite anion exchange membrane for acid recovery by diffusion dialysis, *J. Membr. Sci.*, 2020, 118331.
14 C. Sarkar, C. Bora and S. K. Dolui, Selective dye adsorption by pH modulation on amine-functionalized reduced graphene oxide–carbon nanotube hybrid, *Ind. Eng. Chem. Res.*, 2014, **53**, 16148–16155.
15 S. K. Raj and V. Kulshrestha, Progress in 2D nanomaterial composites membranes for water purification and desalination, in *2D Nanomaterials for Energy and Environmental Sustainability*, Springer Nature Singapore, Singapore, 2022, pp. 125–148.

16 R. R. Ramlal and S. K. Raj, Adsorbents for water desalination, in *Advances in Desalination Insights*, IntechOpen, 2024.
17 S. K. Raj, G. R. Bhadu, P. Upadhyay and V. Kulshrestha, Three-dimensional Ni/Fe doped graphene oxide@MXene architecture as an efficient water splitting electrocatalyst, *Int. J. Hydrogen Energy*, 2022, **47**, 41772–41782.
18 S. Li, L. Wang, J. Peng, M. Zhai and W. Shi, Efficient thorium(IV) removal by two-dimensional Ti_2CT_x MXene from aqueous solution, *Chem. Eng. J.*, 2019, **366**, 192–199.
19 M. Ghidiu, M. Naguib, C. Shi, O. Mashtalir, L. M. Pan, B. Zhang, J. Yang, Y. Gogotsi, S. J. Billinge and M. W. Barsoum, Synthesis and characterization of two-dimensional Nb_4C_3 (MXene), *Chem. Commun.*, 2014, **50**, 9517–9520.
20 J. L. Hart, K. Hantanasirisakul, A. C. Lang, B. Anasori, Y. Gogotsi and M. L. Taheri, Direct correlation of MXene surface chemistry and electronic properties, *Microsc. Microanal.*, 2018, **24**, 1606–1607.
21 M. Naguib, O. Mashtalir, J. Carle, V. Presser, J. Lu, L. Hultman, Y. Gogotsi and M. W. Barsoum, Two-dimensional transition metal carbides, *ACS Nano*, 2012, **6**, 1322–1331.
22 A. Byeon, A. M. Glushenkov, B. Anasori, P. Urbankowski, J. Li, B. W. Byles, B. Blake, K. L. Van Aken, S. Kota, E. Pomerantseva and J.-W. Lee, Lithium-ion capacitors with 2D Nb_2CT_x (MXene)–carbon nanotube electrodes, *J. Power Sources*, 2016, **326**, 686–694.
23 G. Ying, S. Kota, A. D. Dillon, A. T. Fafarman and M. W. Barsoum, Conductive transparent V_2CT_x (MXene) films, *FlatChem*, 2018, **8**, 25–30.
24 A. Hojjati-Najafabadi, M. Mansoorianfar, T. Liang, K. Shahin, Y. Wen, A. Bahrami, C. Karaman, N. Zare, H. Karimi-Maleh and Y. Vasseghian, Magnetic-MXene-based nanocomposites for water and wastewater treatment: a review, *J. Water Proc. Eng.*, 2022, **47**, 102696.
25 L. Ni, W. Sun, J. Mao, J. Lu and H. Wang, The formation potential of disinfection by-products of $Ti_3C_2T_x$ MXene, *J. Water Proc. Eng.*, 2023, **54**, 103944.
26 M. Kurtoglu, M. Naguib, Y. Gogotsi and M. W. Barsoum, First principles study of two-dimensional early transition metal carbides, *MRS Commun.*, 2012, **2**, 133–137.
27 P. Satishkumar, A. M. Isloor and R. Farnood, Fabrication of niobium MXene–polyphenylsulfone membranes: advancement in humic acid and dye separation from wastewater, *J. Water Proc. Eng.*, 2025, **70**, 106985.
28 S. K. Raj, K. B. Patel, V. Sharma, D. N. Srivastava and V. Kulshrestha, Nanopalladium-anchored MXene nanoflowers for boosting electrocatalytic hydrogen evolution reaction, *Energy Fuels*, 2023, **37**, 16856–16865.
29 H. Lin, Y. Chen and J. Shi, Insights into 2D MXenes for versatile biomedical applications: current advances and challenges ahead, *Adv. Sci.*, 2018, **5**, 1800518.
30 F. Du, H. Tang, L. Pan, T. Zhang, H. Lu, J. Xiong, J. Yang and C. J. Zhang, Environmental friendly scalable production of colloidal 2D titanium carbonitride MXene with minimized nanosheets restacking for excellent cycle life lithium-ion batteries, *Electrochim. Acta*, 2017, **235**, 690–699.
31 A. C. Rajan, A. Mishra, S. Satsangi, R. Vaish, H. Mizuseki, K.-R. Lee and A. K. Singh, Machine-learning-assisted accurate band gap predictions of functionalized MXene, *Chem. Mater.*, 2018, **30**, 4031–4038.
32 Y. Y. Peng, B. Akuzum, N. Kurra, M.-Q. Zhao, M. Alhabeb, B. Anasori, E. C. Kumbur, H. N. Alshareef, M.-D. Ger and Y. Gogotsi, All-MXene (2D titanium carbide) solid-state microsupercapacitors for on-chip energy storage, *Energy Environ. Sci.*, 2016, **9**, 2847–2854.
33 Q. Yang, Z. Xu, B. Fang, T. Huang, S. Cai, H. Chen, Y. Liu, K. Gopalsamy, W. Gao and C. Gao, MXene/graphene hybrid fibers for high performance flexible supercapacitors, *J. Mater. Chem. A*, 2017, **5**, 22113–22119.
34 Z. Lu, Y. Wei, J. Deng, L. Ding, Z. K. Li and H. Wang, Self-crosslinked MXene ($Ti_3C_2T_x$) membranes with good antiswelling property for monovalent metal ion exclusion, *ACS Nano*, 2019, **13**, 10535–10544.
35 S. K. Raj, K. Sharma, V. Sharma, T. Ichikawa, A. Jain and V. Kulshrestha, MXene-nanoflower composites as high-performance electrode materials toward solid-state lithium-ion batteries, *Next Energy*, 2025, **9**, 100421.
36 S. K. Raj, Kirti, V. Sharma, D. N. Srivastava and V. Kulshrestha, Single-step synthesis of well-ordered hierarchical nickel nanostructures for boosting the oxygen evolution reaction, *Energy Fuels*, 2022, **36**, 13786–13795.
37 A. Amari, H. S. Aljibori, M. A. Ismail, M. A. Diab, H. A. El-Sabban, A. Umarov, S. Madaminov and N. Elboughdiri, Engineering novel 2D MXene-based dual Z-scheme heterojunction photocatalyst for enhanced TC hydrochloride degradation and hydrogen evolution, *J. Water Proc. Eng.*, 2025, **70**, 107127.
38 W.-T. Cao, C. Ma, D.-S. Mao, J. Zhang, M.-G. Ma and F. Chen, MXene-reinforced cellulose nanofibril inks for 3D-printed smart fibres and textiles, *Adv. Funct. Mater.*, 2019, **29**, 1905898.
39 F. Shahzad, M. Alhabeb, C. B. Hatter, B. Anasori, S.-M. Hong, C. M. Koo and Y. Gogotsi, Electromagnetic interference shielding with 2D transition metal carbides (MXenes), *Science*, 2016, **353**, 1137–1140.
40 R. B. Rakhi, P. Nayak, C. Xia and H. N. Alshareef, Novel amperometric glucose biosensor based on MXene nanocomposite, *Sci. Rep.*, 2016, **6**, 1–10.
41 S. J. Kim, H. J. Koh, C. E. Ren, O. Kwon, K. Maleski, S. Y. Cho, B. Anasori, C. K. Kim, Y. K. Choi, J. Kim and Y. Gogotsi, Metallic $Ti_3C_2T_x$ MXene gas sensors with ultrahigh signal-to-noise ratio, *ACS Nano*, 2018, **12**, 986–993.
42 P. K. Kalambate, N. S. Gadhari, X. Li, Z. Rao, S. T. Navale, Y. Shen, V. R. Patil and Y. Huang, Recent advances in MXene-based electrochemical sensors and biosensors, *TrAC, Trends Anal. Chem.*, 2019, **120**, 115643.
43 C. J. Zhang and V. Nicolosi, Graphene and MXene-based transparent conductive electrodes and supercapacitors, *Energy Storage Mater.*, 2019, **16**, 102–125.

44 Y. Ying, Y. Liu, X. Wang, Y. Mao, W. Cao, P. Hu and X. Peng, Two-dimensional titanium carbide for efficiently reductive removal of highly toxic chromium(VI) from water, *ACS Appl. Mater. Interfaces*, 2015, **7**, 1795–1803.

45 X. Luo, H. Wang, X. Ren, G. Liu, H. Luo, Z. Zheng and F. Wu, Effective adsorptive removal of heavy metal anion Cr(VI) and dye cation methylene blue by the novel 2D material $TiVCT_x$ MXene, *J. Alloys Compd.*, 2025, **1010**, 177409.

46 D.-E. Lee, S. Moru, W. K. Jo and S. Tonda, Sustainable visible-light-induced degradation of antibiotic and dye pollutants using a 2D Ti_3C_2 MXene-supported CoAl-LDH/Bi_2MoO_6 ternary heterostructure with synergistic 2D/2D/2D architecture and S-scheme charge transfer, *J. Water Proc. Eng.*, 2025, **75**, 107868.

47 P. Zhang, L. Wang, K. Du, S. Wang, Z. Huang, L. Yuan, Z. Li, H. Wang, L. Zheng, Z. Chai and W. Shi, Effective removal of U(VI) and Eu(III) by carboxyl functionalized MXene nanosheets, *J. Hazard. Mater.*, 2020, 122731.

48 S. Atri, F. Zazimal, S. Gowrisankaran, Z. Dyrcikova, M. Caplovicova, T. Roch, D. Dvoranova, T. Homola, G. Plesch, M. Brigante and O. Monfort, MXene-decorated spinel oxides as innovative activators of peroxymonosulfate for degradation of caffeine in WWTP effluents: insights into mechanisms, *Chem. Eng. J.*, 2024, **502**, 157814.

49 R. P. Pandey, K. Rasool, V. E. Madhavan, B. Aïssa, Y. Gogotsi and K. A. Mahmoud, Ultrahigh-flux and fouling-resistant membranes based on layered silver/MXene ($Ti_3C_2T_x$) nanosheets, *J. Mater. Chem. A*, 2018, **6**, 3522–3533.

50 S. K. Raj, V. Sharma, S. Mishra and V. Kulshrestha, MoS_2 quantum dot-modified MXene nanoflowers for efficient electrocatalytic hydrogen evolution reaction, *RSC Appl. Interfaces*, 2024, **1**, 1057–1068.

51 S. K. Raj, V. Sharma, D. N. Srivastava and V. Kulshrestha, In-situ evolution of bimetallic Fe/Ni/Co nanohybrids on MXene for improved electrocatalytic oxygen evolution reaction, *Int. J. Hydrogen Energy*, 2023, **48**, 37732–37745.

52 B. Soundiraraju and B. K. George, Two-dimensional titanium nitride (Ti_2N) MXene: synthesis, characterization, and potential application as surface-enhanced Raman scattering substrate, *ACS Nano*, 2017, **11**, 8892–8900.

53 M. Naguib, V. N. Mochalin, M. W. Barsoum and Y. Gogotsi, MXenes: a new family of two-dimensional materials, *Adv. Mater.*, 2014, **26**, 992–1005.

54 A. Sinha, H. Zhao, Y. Huang, X. Lu, J. Chen and R. Jain, MXene: an emerging material for sensing and biosensing, *TrAC, Trends Anal. Chem.*, 2018, **105**, 424–435.

55 X. Yu, X. Cai, H. Cui, S. W. Lee, X.-F. Yu and B. Liu, Fluorine-free preparation of titanium carbide MXene quantum dots with high near-infrared photothermal performances for cancer therapy, *Nanoscale*, 2017, **9**, 17859–17864.

56 F. Han, S. Luo, L. Xie, J. Zhu, W. Wei, X. Chen, F. Liu, W. Chen, J. Zhao, L. Dong and K. Yu, Boosting the yield of MXene 2D sheets *via* a facile hydrothermal-assisted intercalation, *ACS Appl. Mater. Interfaces*, 2019, **11**, 8443–8452.

57 S. Iravani, MXenes and MXene-based (nano)structures: a perspective on greener synthesis and biomedical prospects, *Ceram. Int.*, 2022, **48**, 24144–24156.

58 U. U. Rahman, M. Humayun, U. Ghani, M. Usman, H. Ullah, A. Khan, N. M. El-Metwaly and A. Khan, MXenes as emerging materials: synthesis, properties, and applications, *Molecules*, 2022, **27**, 4909.

59 M. Li, J. Lu, K. Luo, Y. Li, K. Chang, K. Chen, J. Zhou, J. Rosen, L. Hultman, P. Eklund and P. O. Å. Persson, Element replacement approach by reaction with Lewis acidic molten salts to synthesize nanolaminated MAX phases and MXenes, *J. Am. Chem. Soc.*, 2019, **141**, 4730–4737.

60 Y. Li, H. Shao, Z. Lin, J. Lu, L. Liu, B. Duployer, P. O. Å. Persson, P. Eklund, L. Hultman, M. Li and K. Chen, A general Lewis acidic etching route for preparing MXenes with enhanced electrochemical performance in non-aqueous electrolyte, *Nat. Mater.*, 2020, **19**, 894–899.

61 K. R. G. Lim, M. Shekhirev, B. C. Wyatt, B. Anasori, Y. Gogotsi and Z. W. Seh, Fundamentals of MXene synthesis, *Nat. Synth.*, 2022, **1**, 601–614.

62 V. Kamysbayev, A. S. Filatov, H. Hu, X. Rui, F. Lagunas, D. Wang, R. F. Klie and D. V. Talapin, Covalent surface modifications and superconductivity of two-dimensional metal carbide MXenes, *Science*, 2020, **369**, 979–983.

63 P. Huang and W. Q. Han, Recent advances and perspectives of Lewis acidic etching route: an emerging preparation strategy for MXenes, *Nano-Micro Lett.*, 2023, **15**, 68.

64 U. Khan, Y. Luo, L. B. Kong and W. Que, Synthesis of fluorine-free MXene through Lewis acidic etching for application as electrode of proton supercapacitors, *J. Alloys Compd.*, 2022, **926**, 166903.

65 D. Gao, Y. Xu, Z. Liu, Y. Yu, C. Yu, Y. Fang, Y. Huang, C. Tang and Z. Guo, Understanding of strain effect on Mo-based MXenes for electrocatalytic CO_2 reduction, *Appl. Surf. Sci.*, 2024, **654**, 159501.

66 B. Abussaud, H. A. Asmaly, T. A. Saleh, M. A. Atieh and V. K. Gupta, Sorption of phenol from waters on activated carbon impregnated with iron oxide, aluminum oxide and titanium oxide, *J. Mol. Liq.*, 2016, **213**, 351–359.

67 P. Zhao, M. Jian, Q. Zhang, R. Xu, R. Liu, X. Zhang and H. Liu, A new paradigm of ultrathin 2D nanomaterial adsorbents in aqueous media: graphene and GO, MoS_2, MXenes, and 2D MOFs, *J. Mater. Chem. A*, 2019, **7**, 16598–16621.

68 K. M. Lee, C. P. Wong, T. L. Tan and C. W. Lai, Functionalized carbon nanotubes for adsorptive removal of water pollutants, *Mater. Sci. Eng., B*, 2018, **236**, 61–69.

69 S. Wang, H. Sun, H. M. Ang and M. O. Tadé, Adsorptive remediation of environmental pollutants using novel graphene-based nanomaterials, *Chem. Eng. J.*, 2013, **226**, 336–347.

70 P. D. Indurkar, S. K. Raj and V. Kulshrestha, Multivariate modeling and process optimization of Hg(II) remediation using solvothermal synthesized 2D MX/Fe_3O_4 by response

surface methodology: characteristics and mechanism study, *Environ. Sci. Pollut. Res.*, 2023, **30**, 76085–76103.
71 E. Vunain, A. K. Mishra and B. B. Mamba, Dendrimers, mesoporous silicas and chitosan-based nanosorbents for the removal of heavy-metal ions: a review, *Int. J. Biol. Macromol.*, 2016, **86**, 570–586.
72 G. Zou, J. Guo, Q. Peng, A. Zhou, Q. Zhang and B. Liu, Synthesis of urchin-like rutile titania carbon nanocomposites by iron-facilitated phase transformation of MXene for environmental remediation, *J. Mater. Chem. A*, 2016, **4**, 489–499.
73 Q. Peng, J. Guo, Q. Zhang, J. Xiang, B. Liu, A. Zhou, R. Liu and Y. Tian, Unique lead adsorption behavior of activated hydroxyl groups in two-dimensional titanium carbide, *J. Am. Chem. Soc.*, 2014, **136**, 4113–4116.
74 X. Huang, R. Wang, T. Jiao, G. Zou, F. Zhan, J. Yin, L. Zhang, J. Zhou and Q. Peng, Facile preparation of hierarchical AgNP-loaded MXene/Fe_3O_4/polymer nanocomposites by electrospinning with enhanced catalytic performance for wastewater treatment, *ACS Omega*, 2019, **4**, 1897–1906.
75 L. Jin, L. Chai, W. Yang, H. Wang and L. Zhang, Two-dimensional titanium carbides ($Ti_3C_2T_x$) functionalized by poly(m-phenylenediamine) for efficient adsorption and reduction of hexavalent chromium, *Int. J. Environ. Res. Public Health*, 2020, **17**, 167.
76 Q. Zhang, J. Teng, G. Zou, Q. Peng, Q. Du, T. Jiao and J. Xiang, Efficient phosphate sequestration for water purification by unique sandwich-like MXene/magnetic iron oxide nanocomposites, *Nanoscale*, 2016, **8**, 7085–7093.
77 P. Govil, G. Reddy and A. Krishna, Contamination of soil due to heavy metals in the Patancheru industrial development area, Andhra Pradesh, India, *Environ. Geol.*, 2001, **41**, 461–469.
78 N. K. Srivastava and C. B. Majumder, Novel biofiltration methods for the treatment of heavy metals from industrial wastewater, *J. Hazard. Mater.*, 2008, **151**, 1–8.
79 R. Singh, N. Gautam, A. Mishra and R. Gupta, Heavy metals and living systems: an overview, *Indian J. Pharmacol.*, 2011, **43**, 246.
80 F. A. Al-Khaldi, B. Abusharkh, M. Khaled, M. A. Atieh, M. S. Nasser, T. A. Saleh, S. Agarwal, I. Tyagi and V. K. Gupta, Adsorptive removal of cadmium(II) ions from liquid phase using acid-modified carbon-based adsorbents, *J. Mol. Liq.*, 2015, **204**, 255–263.
81 T. S. Anirudhan and S. S. Sreekumari, Adsorptive removal of heavy metal ions from industrial effluents using activated carbon derived from waste coconut buttons, *J. Environ. Sci.*, 2011, **23**, 1989–1998.
82 J. Chen, Q. Huang, H. Huang, L. Mao, M. Liu, X. Zhang and Y. Wei, Recent progress and advances in the environmental applications of MXene-related materials, *Nanoscale*, 2020, **12**, 3574–3592.
83 B. M. Jun, C. M. Park, J. Heo and Y. Yoon, Adsorption of Ba^{2+} and Sr^{2+} on $Ti_3C_2T_x$ MXene in model fracking wastewater, *J. Environ. Manage.*, 2020, **256**, 109940.
84 G. Zhang, T. Wang, Z. Xu, M. Liu, C. Shen and Q. Meng, Synthesis of amino-functionalized $Ti_3C_2T_x$ MXene by alkalization–grafting modification for efficient lead adsorption, *Chem. Commun.*, 2020, **56**, 11283–11286.
85 Y. Tang, C. Yang and W. Que, A novel two-dimensional accordion-like titanium carbide (MXene) for adsorption of Cr(VI) from aqueous solution, *J. Adv. Dielectr.*, 2018, **8**, 1850035.
86 A. K. Fard, G. McKay, R. Chamoun, T. Rhadfi, H. Preud'Homme and M. A. Atieh, Barium removal from synthetic natural and produced water using MXene as two-dimensional nanosheet adsorbent, *Chem. Eng. J.*, 2017, **317**, 331–342.
87 X. Feng, Z. Yu, R. Long, X. Li, L. Shao, H. Zeng, G. Zeng and Y. Zuo, Self-assembling 2D/2D (MXene/LDH) materials achieve ultra-high adsorption of heavy metals Ni^{2+} through terminal group modification, *Sep. Purif. Technol.*, 2020, 117525.
88 X. Sha, H. Huang, S. Sun, H. Huang, Q. Huang, Z. He, M. Liu, N. Zhou, X. Zhang and Y. Wei, Mussel-inspired preparation of MXene–PDA–Bi_6O_7 composites for efficient adsorptive removal of iodide ions, *J. Environ. Chem. Eng.*, 2020, 104261.
89 D. Gan, Q. Huang, J. Dou, H. Huang, J. Chen, M. Liu, Y. Wen, Z. Yang, X. Zhang and Y. Wei, Bioinspired functionalization of MXenes ($Ti_3C_2T_x$) with amino acids for efficient removal of heavy metal ions, *Appl. Surf. Sci.*, 2020, **504**, 144603.
90 L. He, D. Huang, Z. He, X. Yang, G. Yue, J. Zhu, D. Astruc and P. Zhao, Nanoscale zero-valent iron intercalated 2D titanium carbides for removal of Cr(VI) in aqueous solution and the mechanistic aspect, *J. Hazard. Mater.*, 2020, **388**, 121761–121770.
91 A. Shahzad, K. Rasool, W. Miran, M. Nawaz, J. Jang, K. A. Mahmoud and D. S. Lee, Mercuric ion capturing by recoverable titanium carbide magnetic nanocomposite, *J. Hazard. Mater.*, 2018, **344**, 811–818.
92 A. R. Khan, S. K. Awan, S. M. Husnain, N. Abbas, D. H. Anjum, N. Abbas, M. Benaissa, C. R. Mirza, S. Mujtaba-ul-Hassan and F. Shahzad, 3D flower-like δ-MnO_2/MXene nano-hybrids for the removal of hexavalent Cr from wastewater, *Ceram. Int.*, 2021, **47**, 25951–25958.
93 L. Wang, Z. Li, Q. Wu, Z. Huang, L. Yuan, Z. Chai and W. Shi, Layered structure-based materials: challenges and opportunities for radionuclide sequestration, *Environ. Sci.: Nano*, 2020, **7**, 724–752.
94 P. Zhang, L. Wang, L. Yuan, J. Lan, Z. Chai and W. Shi, Sorption of Eu(III) on MXene-derived titanate structures: the effect of nano-confined space, *Chem. Eng. J.*, 2019, **370**, 1200–1209.
95 L. Wang, H. Song, L. Wang, Z. Li, Q. Wu, Z. Huang, L. Yuan, Z. Chai and W. Shi, Efficient U(VI) reduction and sequestration by Ti_2C T_x MXene, *Environ. Sci. Technol.*, 2018, **52**, 10748–10756.
96 I. Ihsanullah, MXenes (two-dimensional metal carbides) as emerging nanomaterials for water purification: progress, challenges and prospects, *Chem. Eng. J.*, 2020, **388**, 124340.
97 S. K. Hwang, S. M. Kang, M. Rethinasabapathy, C. Roh and Y. S. Huh, MXene: an emerging two-dimensional layered

material for removal of radioactive pollutants, *Chem. Eng. J.*, 2020, 125428.

98 L. Wang, W. Tao, L. Yuan, Z. Liu, Q. Huang, Z. Chai, J. K. Gibson, W. Shi and M. W. Barsoum, Loading actinides in multilayered structures for nuclear waste treatment: the first case study of uranium capture with vanadium carbide MXene, *ACS Appl. Mater. Interfaces*, 2016, **8**, 16396–16403.

99 Y. J. Zhang, Z. J. Zhou, J. H. Lan, C. C. Ge, Z. F. Chai, P. Zhang and W. Q. Shi, Theoretical insights into the uranyl adsorption behavior on vanadium carbide MXene, *Appl. Surf. Sci.*, 2017, **426**, 572–578.

100 A. R. Khan, S. M. Husnain, F. Shahzad, S. Mujtaba-ul-Hassan, M. Mehmood, J. Ahmad, M. T. Mehran and S. Rahman, Two-dimensional transition metal carbide ($Ti_3C_2T_x$) as an efficient adsorbent to remove cesium (Cs^+), *Dalton Trans.*, 2019, **48**, 11803–11812.

101 A. Shahzad, M. Moztahida, K. Tahir, B. Kim, H. Jeon, A. A. Ghani, N. Maile, J. Jang and D. S. Lee, Highly effective Prussian blue-coated MXene aerogel spheres for selective removal of cesium ions, *J. Nucl. Mater.*, 2020, 152277.

102 B. M. Jun, M. Jang, C. M. Park, J. Han and Y. Yoon, Selective adsorption of Cs^+ by MXene ($Ti_3C_2T_x$) from model low-level radioactive wastewater, *Nucl. Eng. Technol.*, 2020, **52**, 1201–1207.

103 W. Mu, S. Du, X. Li, Q. Yu, H. Wei, Y. Yang and S. Peng, Removal of radioactive palladium based on novel 2D titanium carbides, *Chem. Eng. J.*, 2019, **358**, 283–290.

104 L. Wang, W. Tao, L. Yuan, Z. Liu, Q. Huang, Z. Chai, J. K. Gibson and W. Shi, Rational control of the interlayer space inside two-dimensional titanium carbides for highly efficient uranium removal and imprisonment, *Chem. Commun.*, 2017, **53**, 12084–12087.

105 Z. He, D. Huang, G. Yue, J. Zhu and P. Zhao, Ca^{2+} induced 3D porous MXene gel for continuous removal of phosphate and uranium, *Appl. Surf. Sci.*, 2021, **570**, 150804.

106 S. Wang, L. Wang, Z. Li, P. Zhang, K. Du, L. Yuan, S. Ning, Y. Wei and W. Shi, Highly efficient adsorption and immobilization of U(VI) from aqueous solution by alkalized MXene-supported nanoscale zero-valent iron, *J. Hazard. Mater.*, 2021, **408**, 124949.

107 M. T. Yagub, T. K. Sen, S. Afroze and H. M. Ang, Dye and its removal from aqueous solution by adsorption: a review, *Adv. Colloid Interface Sci.*, 2014, **209**, 172–184.

108 E. Forgacs, T. Cserhati and G. Oros, Removal of synthetic dyes from wastewaters: a review, *Environ. Int.*, 2004, **30**, 953–971.

109 M. Zubair, N. Jarrah, A. Khalid, M. S. Manzar, T. S. Kazeem and M. A. Al-Harthi, Starch-NiFe-layered double hydroxide composites: efficient removal of methyl orange from aqueous phase, *J. Mol. Liq.*, 2018, **249**, 254–264.

110 A. Khalid and M. Zubair, A comparative study on the adsorption of Eriochrome Black T dye from aqueous solution on graphene and acid-modified graphene, *Arabian J. Sci. Eng.*, 2018, **43**, 2167–2179.

111 K. Vikrant, B. S. Giri, N. Raza, K. Roy, K. H. Kim, B. N. Rai and R. S. Singh, Recent advancements in bioremediation of dye: current status and challenges, *Bioresour. Technol.*, 2018, **253**, 355–367.

112 C. Peng, P. Wei, X. Chen, Y. Zhang, F. Zhu, Y. Cao, H. Wang, H. Yu and F. Peng, A hydrothermal etching route to synthesis of 2D MXene (Ti_3C_2, Nb_2C): enhanced exfoliation and improved adsorption performance, *Ceram. Int.*, 2018, **44**, 18886–18893.

113 O. Mashtalir, K. M. Cook, V. N. Mochalin, M. Crowe, M. W. Barsoum and Y. Gogotsi, Dye adsorption and decomposition on two-dimensional titanium carbide in aqueous media, *J. Mater. Chem. A*, 2014, **2**, 14334–14338.

114 S. Luo, R. Wang, J. Yin, T. Jiao, K. Chen, G. Zou, L. Zhang, J. Zhou, L. Zhang and Q. Peng, Preparation and dye degradation performances of self-assembled MXene-Co_3O_4 nanocomposites synthesized *via* solvothermal approach, *ACS Omega*, 2019, **4**, 3946–3953.

115 K. Li, G. Zou, T. Jiao, R. Xing, L. Zhang, J. Zhou, Q. Zhang and Q. Peng, Self-assembled MXene-based nanocomposites *via* layer-by-layer strategy for elevated adsorption capacities, *Colloids Surf., A*, 2018, **553**, 105–113.

116 Z. Wei, Z. Peigen, T. Wubian, Q. Xia, Z. Yamei and S. ZhengMing, Alkali treated $Ti_3C_2T_x$ MXenes and their dye adsorption performance, *Mater. Chem. Phys.*, 2018, **206**, 270–276.

117 C. Cai, R. Wang, S. Liu, X. Yan, L. Zhang, M. Wang, Q. Tong and T. Jiao, Synthesis of self-assembled phytic acid-MXene nanocomposites *via* a facile hydrothermal approach with elevated dye adsorption capacities, *Colloids Surf., A*, 2020, **589**, 124468.

118 Y. Cui, M. Liu, H. Huang, M. Zhang, D. J. Chen, L. Mao, N. Zhou, F. Deng, X. Zhang and Y. Wei, A novel one-step strategy for preparation of Fe_3O_4-loaded Ti_3C_2 MXenes with high efficiency for removal organic dyes, *Ceram. Int*, 2020, **8**, 11593–11601.

119 Y. Lei, Y. Cui, Q. Huang, J. Dou, D. Gan, F. Deng, M. Liu, X. Li, X. Zhang and Y. Wei, Facile preparation of sulfonic groups functionalized MXenes for efficient removal of methylene blue, *Ceram. Int.*, 2019, **45**, 17653–17661.

120 B. M. Jun, J. Heo, N. Taheri-Qazvini, C. M. Park and Y. Yoon, Adsorption of selected dyes on $Ti_3C_2T_x$ MXene and Al-based metal-organic framework, *Ceram. Int.*, 2020, **46**, 2960–2968.

121 T. Le, E. Jamshidi, M. Beidaghi and M. R. Esfahani, Functionalized-MXene thin-film nanocomposite hollow fiber membranes for enhanced PFAS removal from water, *ACS Appl. Mater. Interfaces*, 2022, **14**, 25397–25408.

122 A. Spyrou, D. Vlastos and M. Antonopoulou, Evidence on the genotoxic and ecotoxic effects of PFOA, PFOS and their mixture on human lymphocytes and bacteria, *Environ. Res.*, 2024, **248**, 118298.

123 F. Dixit, G. Munoz, M. Mirzaei, B. Barbeau, J. Liu, S. V. Duy, S. Sauvé, B. Kandasubramanian and M. Mohseni, Removal of zwitterionic PFAS by MXenes: comparisons with anionic, nonionic, and PFAS-specific resins, *Environ. Sci. Technol.*, 2022, **56**, 6212–6222.

124 J. A. Kemper, E. Sharp, S. Yi, E. M. Leitao, L. P. Padhye, M. Kah, J. L. Chen and K. Gobindlal, Public perceptions of per- and polyfluoroalkyl substances (PFAS): psycho-

demographic characteristics differentiating PFAS knowledge and concern, *J. Cleaner Prod.*, 2024, **442**, 140866.
125 S. Zahmatkesh, Z. Chen, N. A. Khan and B. J. Ni, Removing polyfluoroalkyl substances (PFAS) from wastewater with mixed matrix membranes, *Sci. Total Environ.*, 2023, 168881.
126 B. Shrestha, M. Ezazi, S. Seo, U. Sim, D. H. Lee and G. Kwon, Electrosorption-driven remediation of PFAS-contaminated water using a MXene nanosheet-PEDOT:PSS adsorbent, *ACS Appl. Eng. Mater.*, 2024, **2**, 368–375.
127 Q. Ma, J. Gao, B. Moussa, J. Young, M. Zhao and W. Zhang, Electrosorption, desorption, and oxidation of perfluoroalkyl carboxylic acids (PFCAs) *via* MXene-based electrocatalytic membranes, *ACS Appl. Mater. Interfaces*, 2023, **15**, 29149–29159.
128 J. Zhao, Y. Fan, J. Zhangle and C. Ni, Electrosorption approach removing PFOA from wastewater using a MXene-polyaniline film, *J. Water Proc. Eng.*, 2024, **62**, 105415.
129 Y. Ye, J. M. Steigerwald, H. Bang, V. Jones, K. Dennehy and J. R. Ray, H_2O_2-catalyzed defluorination of perfluorooctanesulfonate (PFOS) by oxidized vanadium carbide MXene nanosheets, *J. Mater. Chem. A*, 2023, **11**, 16803–16814.
130 H. Yang, M. Han, W. Zhang, M. Yi, L. Xia, F. Meng, Y. Wang and S. Zhao, High performance mixed-dimensional assembled MXene composite membranes for molecular sieving, *J. Membr. Sci.*, 2024, **698**, 122606.
131 L. Yang, X. Cao, J. Cui, Y. Wang, Z. Zhu, H. Sun, W. Liang, J. Li and A. Li, Holey Ti_3C_2 nanosheets based membranes for efficient separation and removal of microplastics from water, *J. Colloid Interface Sci.*, 2022, **617**, 673–682.
132 M. Ouda, R. P. Pandey, E. Ouda and S. W. Hasan, Mechanistic insights of nanoplastic-rich water treatment using multi-layer $Ti_3C_2T_x$ electro-membrane filtration and performance prediction, *Chem. Eng. J.*, 2024, 52951.
133 M. Urso, M. Ussia, F. Novotný and M. Pumera, Trapping and detecting nanoplastics by MXene-derived oxide microrobots, *Nat. Commun.*, 2022, **13**, 3573.
134 B. Cao, S. Wan, Y. Wang, H. Guo, M. Ou and Q. Zhong, Highly-efficient visible-light-driven photocatalytic H_2 evolution integrated with microplastic degradation over MXene/$Zn_xCd_{1-x}S$ photocatalyst, *J. Colloid Interface Sci.*, 2022, **605**, 311–319.
135 F. Yang, J. Li, J. Dong, S. Chen, W. Hu, Y. Zhang, H. Wang, Z. Li and Z. Wang, MX@MIL-125(Ti)-mediated sonocatalytic degradation for the dyes and microplastics, *Sep. Purif. Technol.*, 2024, **337**, 126488.
136 S. González-Poggini, A. Rosenkranz and M. Colet-Lagrille, Two-dimensional nanomaterials for the removal of pharmaceuticals from wastewater: a critical review, *Processes*, 2021, **9**, 2160.
137 A. Grzegórska, I. Wysocka, P. Głuchowski, J. Ryl, J. Karczewski and A. Zielińska-Jurek, Novel composite of Zn/Ti-layered double hydroxide coupled with MXene for the efficient photocatalytic degradation of pharmaceuticals, *Chemosphere*, 2022, **308**, 136191.
138 M. Khatami and S. Iravani, MXenes and MXene-based materials for the removal of water pollutants: challenges and opportunities, *Comments Inorg. Chem.*, 2021, **41**, 213–248.
139 A. Shahzad, K. Rasool, M. Nawaz, W. Miran, J. Jang, M. Moztahida, K. A. Mahmoud and D. S. Lee, Heterostructural $TiO_2/Ti_3C_2T_x$ (MXene) for photocatalytic degradation of antiepileptic drug carbamazepine, *Chem. Eng. J.*, 2018, **349**, 748–755.
140 S. Kim, F. Gholamirad, M. Yu, C. M. Park, A. Jang, M. Jang, N. Taheri-Qazvini and Y. Yoon, Enhanced adsorption performance for selected pharmaceutical compounds by sonicated $Ti_3C_2T_x$ MXene, *Chem. Eng. J.*, 2021, **406**, 126789.
141 X. Liu and C. Chen, MXene enhanced the photocatalytic activity of ZnO nanorods under visible light, *Mater. Lett.*, 2020, **261**, 127127.
142 P. Zhang, M. Xiang, H. Liu, C. Yang and S. Deng, Novel two-dimensional magnetic titanium carbide for methylene blue removal over a wide pH range: insight into removal performance and mechanism, *ACS Appl. Mater. Interfaces*, 2019, **11**, 24027–24036.
143 A. Bina and H. Raissi, A strategy to improve the adsorption capacity of OPs-dye pollutants from the aqueous environment using adsorbents based on 2D transition metal carbides (V_2CT_x), *Appl. Water Sci.*, 2025, **15**, 10.
144 H. Lei, Z. Hao, K. Chen, Y. Chen, J. Zhang, Z. Hu, Y. Song, P. Rao and Q. Huang, Insight into adsorption performance and mechanism on efficient removal of methylene blue by accordion-like V_2CT_x MXene, *J. Phys. Chem. Lett.*, 2020, **11**, 4253–4260.
145 S. Atri, V. V. Kusumkar, S. İnan, M. Gregor, T. Roch, M. Caplovicova, M. Galambos, E. Viglasova, G. Plesch, M. Motola and O. Monfort, Fe_3O_4-decorated MXene for the effective removal of ^{133}Ba and ^{137}Cs: synthesis, characterization, and optimization *via* response surface methodology (RSM), *Inorg. Chem. Front.*, 2024, **11**, 7860–7871.
146 A. A. Perera, K. A. Madhushani, B. T. Punchihewa, A. Kumar and R. K. Gupta, MXene-based nanomaterials for multifunctional applications, *Materials*, 2023, **16**, 1138.
147 A. A. Ghani, A. Shahzad, M. Moztahida, K. Tahir, H. Jeon, B. Kim and D. S. Lee, Adsorption and electrochemical regeneration of intercalated $Ti_3C_2T_x$ MXene for the removal of ciprofloxacin from wastewater, *Chem. Eng. J.*, 2021, **421**, 127780.
148 Y. Dong, D. Sang, C. He, X. Sheng and L. Lei, MXene/alginate composites for lead and copper ion removal from aqueous solutions, *RSC Adv.*, 2019, **9**, 29015–29022.
149 Y. Du, B. Yu, L. Wei, Y. Wang, X. Zhang and S. Ye, Efficient removal of Pb(II) by $Ti_3C_2T_x$ powder modified with a silane coupling agent, *J. Mater. Sci.*, 2019, **54**, 13283–13297.
150 Y. Feng, H. Wang, J. Xu, X. Du, X. Cheng, Z. Du and H. Wang, Fabrication of MXene/PEI functionalized sodium alginate aerogel and its excellent adsorption behavior for Cr(VI) and Congo Red from aqueous solution, *J. Hazard. Mater.*, 2021, **416**, 125777.

151 H. Wan, L. Nan, H. Geng, W. Zhang and H. Shi, Green synthesis of a novel MXene–CS composite applied in treatment of Cr(VI) contaminated aqueous solution, *Processes*, 2021, **9**, 524.

152 X. Hu, C. Chen, D. Zhang and Y. Xue, Kinetics, isotherm and chemical speciation analysis of Hg(II) adsorption over oxygen-containing MXene adsorbent, *Chemosphere*, 2021, **278**, 130206.

153 A. Shahzad, J. Jang, S. R. Lim and D. S. Lee, Unique selectivity and rapid uptake of molybdenum-disulfide-functionalized MXene nanocomposite for mercury adsorption, *Environ. Res.*, 2020, **182**, 109005.

154 W. Mu, S. Du, X. Li, Q. Yu, H. Wei, Y. Yang and S. Peng, Removal of radioactive palladium based on novel 2D titanium carbides, *Chem. Eng. J.*, 2019, **358**, 283–290.

155 A. Shahzad, M. Nawaz, M. Moztahida, K. Tahir, J. Kim, Y. Lim, B. Kim, J. Jang and D. S. Lee, Exfoliation of titanium aluminum carbide (211 MAX phase) to form nanofibers and two-dimensional nanosheets and their application in aqueous-phase cadmium sequestration, *ACS Appl. Mater. Interfaces*, 2019, **11**, 19156–19166.

156 X. Feng, Z. Yu, R. Long, X. Li, L. Shao, H. Zeng, G. Zeng and Y. Zuo, Self-assembling 2D/2D (MXene/LDH) materials achieve ultra-high adsorption of heavy metals Ni^{2+} through terminal group modification, *Sep. Purif. Technol.*, 2020, **253**, 117525.

157 A. K. Fard, T. Rhadfi, G. McKay, Y. Manawi, V. Kochkodan, O. S. Lee and M. A. Atieh, Two-dimensional MXene for efficient arsenic removal from aqueous solutions: experimental and molecular dynamics simulation, Desal, *Water Treat.*, 2021, **211**, 280–295.

158 J. Ren, Z. Zhu, Y. Qiu, F. Yu, T. Zhou, J. Ma and J. Zhao, Enhanced adsorption performance of alginate/MXene/$CoFe_2O_4$ for antibiotic and heavy metal under rotating magnetic field, *Chemosphere*, 2021, **284**, 131284.

159 S. Park, S. Kim, Y. Yea, K. Saravanakumar, E. Lee, Y. Yoon and C. M. Park, Adsorptive and photocatalytic performance of cobalt-doped $ZnTiO_3/Ti_3C_2T_x$ MXene nanohybrids towards tetracycline: kinetics and mechanistic insight, *J. Hazard. Mater.*, 2023, **443**, 130165.

160 X. Wang, A. Zhang, M. Chen, M. K. Seliem, M. Mobarak, Z. Diao and Z. Li, Adsorption of azo dyes and Naproxen by few-layer MXene immobilized with dialdehyde starch nanoparticles: adsorption properties and statistical physics modeling, *Chem. Eng. J.*, 2023, **473**, 145385.

161 Q. Liu, X. Tan, S. Wang, F. Ma, H. Znad, Z. Shen, L. Liu and S. Liu, MXene as a non-metal charge mediator in 2D layered $CdS@Ti_3C_2@TiO_2$ composites with superior Z-scheme visible light-driven photocatalytic activity, *Environ. Sci.: Nano*, 2019, **6**, 3158–3169.

162 B. Shrestha, M. Ezazi, S. Seo, U. Sim, D. H. Lee and G. Kwon, Electrosorption-driven remediation of PFAS-contaminated water using a MXene nanosheet-PEDOT:PSS adsorbent, *ACS Appl. Eng. Mater.*, 2024, **2**, 368–375.

163 S. Kim, F. Gholamirad, M. Yu, C. M. Park, A. Jang, M. Jang, N. Taheri-Qazvini and Y. Yoon, Enhanced adsorption performance for selected pharmaceutical compounds by sonicated $Ti_3C_2T_x$ MXene, *Chem. Eng. J.*, 2021, **406**, 126789.

164 Q. Ma, J. Gao, B. Moussa, J. Young, M. Zhao and W. Zhang, Electrosorption, desorption, and oxidation of perfluoroalkyl carboxylic acids (PFCAs) *via* MXene-based electrocatalytic membranes, *ACS Appl. Mater. Interfaces*, 2023, **15**, 29149–29159.

165 E. M. Ahmed, A. S. Ali, E. M. Hieba, Z. S. Shaban, M. S. Fathy, A. M. Amer, A. M. Ishmael, A. Bakr, H. R. Rashdan and A. Elzwawy, Exploring the potential of MXenes in advanced energy, environmental, and biomedical applications, *RSC Adv.*, 2025, **15**, 44812–44863.

166 M. A. El-Khair, A. O. El Naga, K. Z. Elwakeel, A. M. Elgarahy, A. K. Priya, K. K. Yadav and A. S. Morshedy, The promise of graphene-based photocatalytic materials for wastewater remediation: a scoping review, *Coord. Chem. Rev.*, 2025, **544**, 216961.

167 C. L. Lai, A. Mukundan, R. Karmakar, R. Kaur, K. L. Huang and H. C. Wang, Advances in MoS_2-based biosensors: from material fabrication and characterization to biomedical, environmental, and industrial applications, *Biosens*, 2025, **15**, 371.

168 K. H. Aziz, F. S. Mustafa and S. Hama, Pharmaceutical removal from aquatic environments using multifunctional metal-organic frameworks (MOFs) materials for adsorption and degradation processes: a review, *Coord. Chem. Rev.*, 2025, **542**, 216875.

169 K. H. Aziz, F. S. Mustafa, R. F. Hamarawf and K. M. Omer, Adsorptive removal of toxic heavy metals from aquatic environment by metal-organic framework (MOF): a review, *J. Water Proc. Eng.*, 2025, **70**, 106867.

170 F. Cheng, Y. Wang, C. Cai and Y. Fu, Multiscale MXene Engineering for Enhanced Capacitive Deionization *via* Adaptive Surface Charge Tailoring, *Nano Lett.*, 2024, **24**, 9477–9486.

171 X. Lai, Y. Tang, Y. Dong, Y. Luo, X. Yang and Q. Peng, Multifunctional MXene nanosheets and their applications in antibacterial therapy, *Adv. NanoBiomed Res.*, 2024, **4**, 2400033.

172 Y. Wang, Y. Wang, Y. Kuai and M. Jian, "Visualization" gas–gas sensors based on high performance novel MXenes materials, *Small*, 2024, **20**, 2305250.

173 N. K. Nguyen, S. Lee, Q. D. Nguyen, P. Park, I. J. Yoon and J. Nah, Absorption-dominant electromagnetic interference shielding material using MXene-coated polyvinylidene fluoride foam, *Mater. Today Phys.*, 2024, **46**, 101509.

174 M. Shen, W. Jiang, K. Liang, S. Zhao, R. Tang, L. Zhang and J. Q. Wang, One-pot green process to synthesize MXene with controllable surface terminations using molten salts, *Angew. Chem.*, 2021, **133**, 27219–27224.

175 Y. Wang, B. Zhou, Q. Tang, Y. Yang, B. Pu, J. Bai, J. Xu, Q. Feng, Y. Liu and W. Yang, Ultrafast synthesis of MXenes in minutes *via* low-temperature molten salt etching, *Adv. Mater.*, 2024, **36**, 2410736.

176 M. Z. Abid, K. Rafiq, A. Aslam, R. Jin and E. Hussain, Scope, evaluation and current perspectives of MXene synthesis

strategies for state of the art applications, *J. Mater. Chem. A*, 2024, **12**, 7351–7395.

177 X. Feng, Z. Yu, R. Long, Y. Sun, M. Wang, X. Li, G. Zeng and G. Zuo, Polydopamine intimate contacted two-dimensional/two-dimensional ultrathin nylon basement membrane supported RGO/PDA/MXene composite material for oil–water separation and dye removal, *Sep. Purif. Technol.*, 2020, **247**, 116945.

178 Y. Wei, R. Bao, L. Hu, Y. Geng, X. Chen, Y. Wen, Y. Wang, M. Qin, Y. Zhang and X. Liu, Ti_3C_2 (MXene) nanosheets disrupt spermatogenesis in male mice mediated by the ATM/p53 signaling pathway, *Biol. Direct*, 2023, **18**, 30.

179 I. Soni, M. Ahuja, P. K. Jagtap, V. Chauhan, S. K. Raj and P. P. Sharma, The Advent of MXene-Based Synthetics and Modification Approaches for Advanced Applications in Wastewater Treatment, *Membranes*, 2025, **15**(12), 364.